[American Journal of Science, Vol. 303, December, 2003, P. 865–904]

American Journal of Science

DECEMBER 2003

CHEMOSTRATIGRAPHY OF CARBONATES FROM THE MINAS SUPERGROUP, QUADRILÁTERO FERRÍFERO (IRON QUADRANGLE), BRAZIL: A STRATIGRAPHIC RECORD OF EARLY PROTEROZOIC ATMOSPHERIC, BIOGEOCHEMICAL AND CLIMATIC CHANGE

A. BEKKER*†, A. N. SIAL**, J. A. KARHU***, V. P. FERREIRA**, C. M. NOCE****, A. J. KAUFMAN*****, A. W. ROMANO****, and M. M. PIMENTEL******

ABSTRACT. **The ca. 2.42 Ga-old Gandarela Formation overlies the finely laminated Cauê Banded Iron Formation (BIF) of the Itabira Group, Minas Supergroup, Brazil and consists of red carbonate facies BIF grading upsection into buff dolomites and limestones, which are locally stromatolitic. Carbonates of the Gandarela Formation have $\delta^{13}C$ values ranging narrowly from -1.6 to +0.4 permil versus PDB (n = 93).**

The Cercadinho Formation, at the base of the overlying Piracicaba Group, is a thick arenaceous succession with rare thin carbonates that have $\delta^{13}C$ values ranging from +3.3 to +5.4 permil (n = 12). Stromatolitic dolomites of the overlying Fecho do Funil Formation have Pb-Pb carbonate age 2.11 ± 0.11 Ga (Babinski and others, 1995) that provide the minimum age for this unit and $\delta^{13}C$ values ranging from +5.6 to +7.4 permil (n = 69).

At present, we find no evidence in Brazil for the any of the three early Paleoproterozoic glacial events recognized in 2.45 to 2.22 Ga sedimentary successions in North America. Given the radiometric constraints, however it is possible that geological and geochemical traces of these ice ages are missing along the unconformity between the Gandarela and Cercadinho formations. If correct, carbonates of the Gandarela Formation may provide a record of the carbon isotope composition of the seawater prior to any of the Paleoproterozoic ice ages. Combined with other available $\delta^{13}C$ data results from the Gandarela Formation suggest that seawater preceding the ice ages was not significantly enriched in ^{13}C. On the other hand, the carbon isotopic signature of the Cercadinho carbonates and chemical composition of the Cercadinho arenites are consistent with deposition after the end of the glacial epoch and likely during the early stage of ca. 2.22 to 2.1 Ga carbon isotope excursion. The $\delta^{13}C$ values of marine carbonates of the Fecho do Funil Formation are consistent with carbon isotope record of contemporaneous carbonate successions worldwide providing additional evidence for a global biogeochemical anomaly at ca. 2.22 to 2.1 Ga. These compositional and isotopic changes allow integration of the Minas Supergroup into the global record of the Paleoproterozoic evolution as well as correlation with other successions of similar age.

INTRODUCTION

Proterozoic (2.5 - 0.54 Ga) Earth history is characterized by the presence of remarkable tectonic, environmental, and biologic events at either end of the eon. Both

* Department of Earth and Planetary Sciences, Harvard University, Cambridge, Massachusetts 02138 USA; abekker@fas.harvard.edu
** NEG-LABISE, Department of Geology, UFPE, C.P. 7852, 50670-000, Recife, Brazil
*** Department of Geology, University of Helsinki, P.O. Box 64, FIN-00014, Finland
**** Institute of Geoscience-CPMTC, UFMG, Belo Horizonte, 31270-901, Brazil
***** Department of Geology, University of Maryland at College Park, College Park, Maryland 20742, USA
****** Institute of Geosciences, UnB, Brasilia, D.F., 70910-900, Brazil
† Corresponding author

the beginning (2.45 - 2.0 Ga) and the end (0.75 - 0.54 Ga) are marked by the breakup and assembly of supercontinents (Williams and others, 1991; Hoffman, 1991), as well as extensive (and potentially global) glaciations, which are associated with extreme variations in the carbon isotope composition of seawater proxies. In both intervals a marked decrease in atmospheric CO_2 levels, either through high productivity and burial of organic matter on newly-formed continental margins (Kaufman and others, 1997; Kaufman, 1997; Hoffman and others, 1998) or by long-term enhanced weathering of land masses within middle to low latitudes (Hoffman and Schrag, 2000, 2002) has been inferred to explain 'Snowball Earth' climate conditions.

The carbon isotope composition of Mesoproterozoic carbonates is close to 0 permil but shifts to much higher values before the first Neoproterozoic ice age (Kaufman and others, 1997; Brasier and Lindsay, 1998; Kah and others, 1999). Neoproterozoic ice ages and associated negative carbon isotope excursions were preceded by positive carbon isotope excursions (Hoffman and others, 1998). Positive carbon isotope excursions in seawater composition are generally interpreted as indicating high relative burial rates of organic matter and accompanying increase in the oxygen production (Broecker, 1970; Hayes and others, 1983; Derry and others, 1992; Kaufman and Knoll, 1995; Karhu and Holland, 1996; Kaufman and others, 1997). Kaufman (1997) suggested similar coupling between climatic changes and biogeochemical cycling of carbon for the Paleoproterozoic. It was recently suggested that the Archean and early Paleoproterozoic atmosphere was rich in methane (Hayes, 1994; Kasting, 1998; Rye and Holland, 2000; Pavlov and others, 2000), a greenhouse gas that kept the planet's surface above the freezing point. The transition to the oxidizing atmosphere at ca. 2.4 Ga ago could have decreased the atmospheric methane content resulting in the Paleoproterozoic glacial epoch (Pavlov and others, 2000). Insofar as atmospheric and climatic changes affected surface environments, it should ultimately be possible to test the proposed relationship between the rise of the atmospheric oxygen, ice ages, and biogeochemical anomalies by unraveling the position of these events within continuous or well correlated stratigraphic sections.

The tectonomagmatic event at 2.48 to 2.45 Ga (Heaman, 1997; Kump and others, 2000) led to bimodal magmatism and rifting of the Late Archean supercontinent called *Kenorland* (Williams and others, 1991), while open continental margins were affected by predominantly mafic volcanism accompanied by deposition of BIFs (Barley and others, 1997). This event was superseded by a compressional event recognized in South Africa, Australia, Antarctica, and Montana, USA (Altermann and Hälbich, 1991; Daly and Fanning, 1993; Krapež, 1996; Bekker and others, 2001a; Carson and others, 2002; Roberts and others, 2002). The compressional event was shortly followed by a glacial epoch that includes a triad of glacial events in North America while on other continents evidence only for two (South Africa), one (Fennoscandia) or none of these events is found (Young, 1973; Ojakangas, 1988; Bekker and others, 2001a). Negative carbon isotope excursion (Veizer and others, 1992a; Bekker and Karhu, 1996; Bekker and others, 1999) marks cap carbonates above the middle of three glacial diamictites in the Snowy Pass and Huronian supergroups, Wyoming and Ontario, respectively. A negative carbon isotope excursion with a similar magnitude and likely similar age was also found in South Africa above the glacial diamictite at the base of the Duitschland Formation (Bekker and others, 2001a).

Until recently, highly positive carbon isotope values (>4‰) were only found in Paleoproterozoic carbonates that are younger than the end of the glacial epoch based on geochronologic age constraints and stratigraphic position (Karhu and Holland, 1996). However, carbonates of the upper Duitschland Formation, South Africa sandwiched between two glacial diamictites have $\delta^{13}C$ values as high as +10.1 permil (Bekker and others, 2001a).

Carbon isotope composition of seawater before and after the first of three Paleoproterozoic ice ages remains poorly constrained. This information is relevant to the question whether the decreased atmospheric CO_2 and CH_4 levels necessary to launch into icehouse conditions were brought by change in the rate of organic matter burial or in the rate of weathering. Karhu and Holland (1996) used $\delta^{13}C$ values of carbonates from the Seidorechka and Gandarela formations in their curve of secular carbon isotope variations. These units based on their stratigraphic position in respect to glacial deposits or absolute ages are older than the triad of glacial events (Pokrovsky and Melezhik, 1995; Karhu and Holland, 1996; Melezhik and others, 1999). The 2442 ± 1.7 Ma Seidorechka Formation in the Imandra-Varzuga Zone of the Kola Peninsula, Russia contains thin impure carbonate lenses in lacustrine arenites (Amelin and others, 1995; Pokrovsky and Melezhik, 1995). The Seidorechka Formation was deposited in a rift basin with subaerial volcanic activity (Melezhik and Sturt, 1994) and was subjected to metamorphism of greenschist to amphibole facies (Melezhik and others, 1997a). The overlying Polisarka Formation contains dropstones (Melezhik, 1992 in Sturt and others, 1994) suggesting glacial influence on deposition. Carbonates have $\delta^{13}C$ values ranging from -4.8 to -1.8 permil with dolomites being less depleted (Karhu and Melezhik, 1992; Pokrovsky and Melezhik, 1995; Melezhik and Fallick, 1996). Lithostratigraphy, depositional environment and geochemical data suggest that the highly depleted carbon isotope values reflect either local environment or diagenetic / metamorphic alteration and can not be used for the curve of secular carbon isotope variations.

The 2420 ± 19 Ma Gandarela Formation, Minas Supergroup, Brazil was deposited on a passive continental margin (Dorr, 1969; Romano, ms, 1989; Babinski and others, 1995). Glacial diamictites are not known in the Minas Supergroup. Carbon isotope values of carbonates and total organic carbon (TOC) from the Gandarela Formation measured by Schidlowski and others (1976a) and, recently, by Sial and others (1999, 2000) range from -3.2 to +1.6 and −22.9 to −21.4 permil, respectively.

Recently, two other successions provided information relevant to the carbon isotope composition of the Paleoproterozoic seawater before and after the first glacial event. Lindsay and Brasier (2002) and Bekker and others (2002) studied carbonates of the Turee Creek Group in the Duck Creek and Hardey synclines of the Hamersley Basin, Western Australia. Carbonates from the Hardey syncline overlie glacial diamictites of the Meteorite Bore Member of the Turee Creek Group, while those in the Duck Creek syncline, based on a *tentative* sequence stratigraphic correlation by Krapež (1996), are older than glacial diamictites of the Meteorite Bore Member. These carbonates have $\delta^{13}C$ values close to 0 permil (see Bekker and others, 2002 for discussion of highly negative carbon isotope values in Lindsay and Brasier, 2002). Bekker and others (2001a) found $\delta^{13}C$ values as high as +3.5 permil in carbonates of the Tongwane Formation that overlies the ca. 2.48 Ga old Penge Iron Formation and unconformably underlies Paleoproterozoic glacial diamictites in South Africa. In summary, these limited data do not resolve ocean $\delta^{13}C$ composition before the triad of Paleoproterozoic glacials.

In North America, Fennoscandia, and South Africa mature hematitic quartzites and Al-rich shales overlie the ultimate Paleoproterozoic diamictite (Young, 1973; Ojakangas, 1988; Bekker and others, 2001a). Chemical and mineralogical composition of these rocks suggests that high atmospheric p_{O_2} and p_{CO_2} along with warm global climate resulted in deep weathering of low-standing landmasses in the aftermath of the Paleoproterozoic glacial epoch. Carbonates are rare on this stratigraphic level and, based on limited data (Yudovich and others, 1990; Tikhomirova and Makarikhin, 1993; Bekker and Karhu, 1997; Bekker and others, unpublished data), have only moderate ^{13}C-enrichment. In contrast, dolomites with remarkably positive carbon isotope values

dominating the >2.22 to 2.06 Ga stratigraphic record (Karhu, 1993; Karhu and Holland, 1996) overlie the horizon of intense weathering. Ubiquitous pseudomorphs of sulfate evaporites in these carbonate successions (Hemzacek and others, 1982; Genest, 1985; Chandler, 1988; Melezhik and Fetisova, 1989; Akhmedov, 1990; Master, 1990; El Tabakh and others, 1999; Melezhik and others, 1999; Bekker and Eriksson, 2003) suggest deposition in a warm arid climate. These ^{13}C-enriched carbonate successions are typically overlain by organic-rich shales containing phosphorite, BIF, and Mn-rich carbonate, which is consistent with the view of enhanced ocean circulation following the long time interval with high relative burial rate of organic carbon (Bekker and others, 2003). The end of the carbon isotope excursion and enhanced ocean circulation were potentially linked to the final breakup of Kenorland at ca. 2.1 Ga, which coincides in age with the mantle plume event (Kohonen, 1995; Aspler and Chiarenzelli, 1998; Aspler and others, 2002).

In this study, we present stratigraphic and carbon isotopic data from the early Paleoproterozoic Minas Supergroup in Brazil, a succession that contains no known glacial record. The succession is unique, however, in that carbonates of the ca. 2.42 Ga Gandarela Formation conformably overlie banded iron-formation of the Cauê Formation. Thus the Gandarela carbonates may reflect seawater and atmospheric composition in the interval just before the Paleoproterozoic glacial epoch. The chemostratigraphic data along with radiometric ages and time-specific rock types are used to correlate the Minas Supergroup with equivalents in South Africa and Australia, and to speculate on causes of the Paleoproterozoic glaciations.

REGIONAL GEOLOGY AND STRATIGRAPHY

The Minas Supergroup is exposed in the southeastern part of the São Francisco Craton in the Quadrilátero Ferrífero, southeast Brazil (fig. 1). It is in fault or unconformable contact with Archean granite-gneiss terrains with a minimum age of 2.86 Ga, the 2.78 to 2.72 Ga old Rio das Velhas greenstone belt, and granite plutons with ages ranging from 2612 to 2780 Ma (Machado and others, 1992; Machado and Carneiro, 1992; Chemale and others, 1994; Noce and others, 1998; Endo and others, 2002). Deposition of the Minas Supergroup initiated with rifting and breakup of the eastern margin on the Archean platform and ended with the Transamazonian Orogeny (Marshak and Alkmim, 1989). The late stage of the Transamazonian Orogeny was constrained by titanite ages of 2059 ± 6 Ma and 2041 ± 6 Ma (Machado and others, 1992; Noce and others, 1998) and by 2125 ± 4 Ma U-Pb age of detrital zircon from the overlying orogenic Sabará Group (Machado and others, 1992).

The supergroup includes the Caraça, Itabira, and Piracicaba groups (Dorr 1969; Renger and others, 1994; fig. 2). Detrital zircons from the lower Moeda Formation of the Caraça Group yield Pb-Pb ages of 2651 ± 33 Ma and 2606 ± 47 Ma revealed by LA-ICPMS techniques (Machado and others, 1996), and an age of ca. 2.61 Ga by U-Pb SHRIMP measurements (Endo and others, 2002). A minimum age constraint for the Itabira Group is provided by the 2420 ± 19 Ma Pb-Pb carbonate age of the Gandarela Formation (Babinski and others, 1995).

The Caraça Group was deposited in a rift associated with thermally subsiding passive margin settings. At the base of the group, the Moeda Formation contains layers and lenses of phyllites in mature quartz arenites and quartz pebble conglomerates with placer deposits of uraninite, gold, and pyrite, indicating deposition under a low oxygen content atmosphere (Villaça and Moura, 1981; Minter and others, 1990). The conformably and, locally, gradationally overlying Batatal Formation contains sericitic and graphitic phyllites, chert, and an iron formation. The phyllites in the upper few meters of this formation are Fe-rich and grade upwards into the Cauê Iron Formation of the Itabira Group.

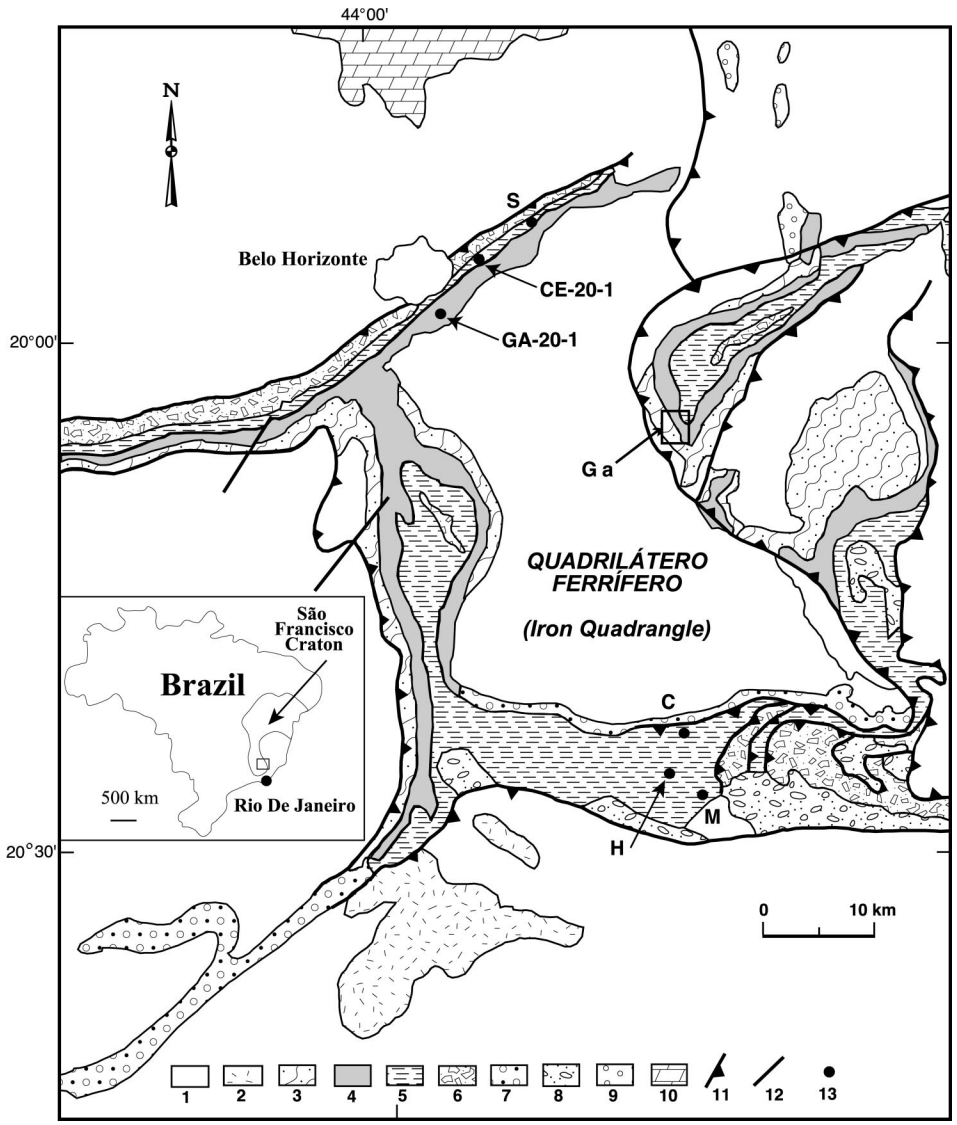

Fig. 1. Schematic geological map (modified from Dorr, 1969) of the Quadrilátero Ferrífero (Iron Quadrangle) area with sampled localities shown. 1 – Archean terrain (granite-gneisses and greenstones); 2 – Paleoproterozoic granitoids; 3 – Caraça Group; 4 – Itabira Group; 5 – Piracicaba Group; 6 – Sabará Group; 7 - Minas Supergroup undivided; 8 – Itacolomi Group; 9 – Mesoproterozoic Espinhaço Supergroup; 10 – Neoproterozoic Bambui Group; 11 – thrust; 12 – fault; 13 – sampled locality (Ga - Gandarela Farm (see fig. 3); H - Hargraves quarry; S - Sabará; C - Cumbi quarry; CE-20-1 and GA-20-1 are in the Curral anticline; and M – Morro do Bule). Inset shows location of the Quadrilátero Ferrífero (Iron Quadrangle) area in Brazil.

The Itabira Group contains the Cauê Iron Formation and the overlying Gandarela Formation. The latter unit has gradational contact with the Cauê Iron Formation and includes dolomites, limestones, dolomitic phyllite, a dolomitic iron formation, and phyllite (Dorr, 1969). Carbonates in the middle part of the Gandarela Formation contain well-preserved domal and LLH-type (laterally-linked hemispheroids of Logan and others, 1964) stromatolites and oncolites (Souza and Müller, 1984), indicating

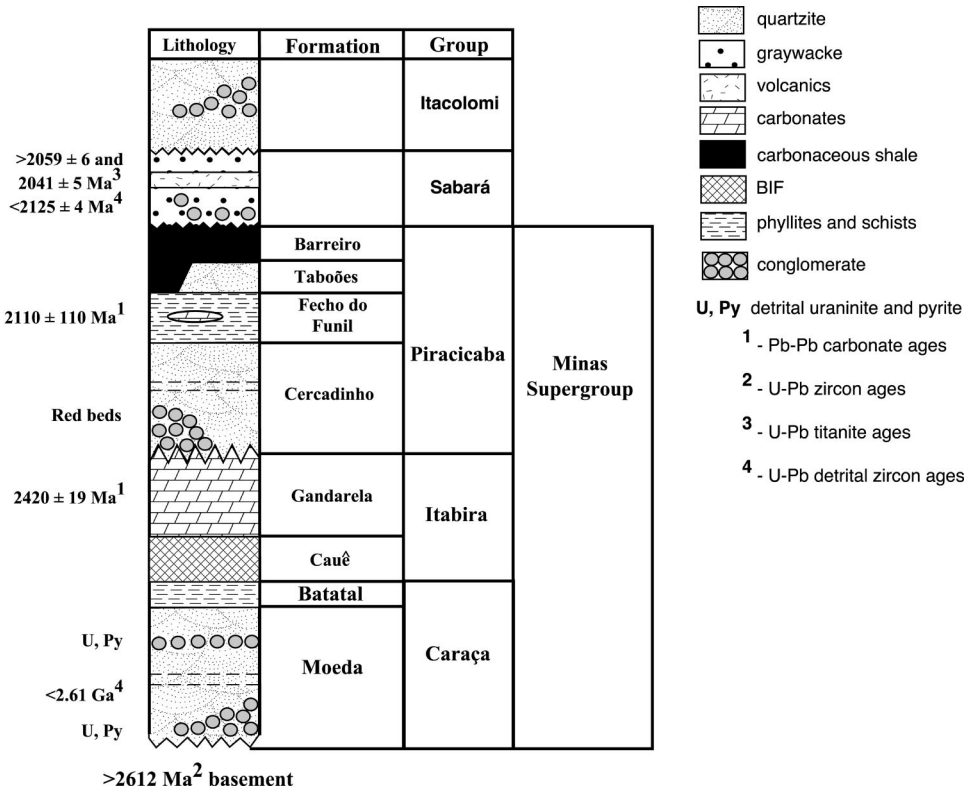

Fig. 2. Stratigraphy of the Minas Supergroup (modified from Dorr, 1969). See text for references to the ages. Thickness of the supergroup is variable throughout the basin with the maximum estimate of 4 km, Sabará Group is more than 3 km thick, and the Itacolomi Group is 1 to 2 km thick (Dorr, 1969).

deposition in high-energy intertidal to shallow subtidal environments. Intraformational dolomite and chert flat-pebble conglomerates, which range in thickness from few centimeters to more than 1meter occur in the upper part of this unit (Dorr, 1969). Dark-colored dolomites contain up to 1.2 percent Mn (Moore, 1969).

The Cercadinho Formation, the lowest unit in the overlying Piracicaba Group, contains quartz arenites, ferruginous phyllites and quartz arenites, and phyllites. Conglomerates at the base of this unit include clasts of BIF and chert derived from the Itabira Group, specularite pebbles and iron-rich concretions (Dorr, 1969). The Cercadinho Formation gradually transects units of the Itabira Group to the west (Dorr, 1969). Other evidence of erosional unconformity include locally angular contact with the Gandarela Formation and locally preserved regolith at the top of the Gandarela Formation containing red or variegated fine-grained lenticular rock (Maxwell, 1972). Phyllites in the basal part of the formation contain large amounts of kyanite, are rich in Al_2O_3, and were interpreted as a reworked Al-rich regolith above the disconformity (Herz, 1962; Herz and Dutra, 1964). The Cercadinho Formation has a variable thickness but in the type locality in the Belo Horizonte Quadrangle it is about 317 meters thick (Dorr, 1969). Coarse- to medium-grained quartz arenites contain well rounded and sorted quartz grains in hematite and magnetite matrix. Analyses of ferruginous quartz arenites show up to 95 percent SiO_2 and up to 12.3 percent Fe_2O_3 (Simmons, 1968; Romano, ms, 1989). Herringbone cross bedding, planar bedding, soft-sediment

deformation structures, and ripple marks are abundant in quartz arenites of the Cercadinho Formation, indicating deposition in a shallow-marine, tidally-influenced setting (Romano, ms, 1989).

The overlying Fecho do Funil Formation has conformable upper and lower contacts. The formation contains phyllite, siltstone, ferruginous quartz arenite, and lenses of argillaceous dolomite. Phyllite is more abundant in the lower part of the formation and dolomite content increases upsection. The Fecho do Funil Formation has a variable thickness but in the type locality near the community of Fecho do Funil it reaches 410 meters in thickness (Simmons, 1968). Dolomite lenses are up to 30 meters thick, contain long columnar and domal stromatolites (Dardenne and Campos Neto, 1975; Garcia and others, 1988) and lack siliciclastic detritus, indicating a subtidal to intertidal depositional setting. The whole formation likely represents a regressive cycle with the deeper-water facies at the base and upward-shallowing trend towards the gradual contact with the Taboões Quartzite. A 2110 ± 110 Ma Pb-Pb carbonate age of the Fecho do Funil Formation was related to a metamorphic overprint due to the Transamazonian event (Babinski and others, 1995). The overlying deltaic Taboões Quartzite consists of cross-bedded equigranular fine-grained quartz arenite and contains up to 98.5 percent SiO_2 (Romano, ms, 1989). The conformably overlying Barreiro Formation contains phyllite and pyrite- and graphite-rich phyllites with TOC content up to 4.4 percent. Since the Taboões Quartzite and Barreiro Formation interfinger on a regional scale and are not present everywhere, they are likely time-equivalent facies (Romano, ms, 1989).

The unconformably overlying ~3 kilometer thick Sabará Group and the 1 to 2 kilometer thick Itacolomi Group contain coarse-grained siliciclastic and volcanic rocks (Renger and others, 1994) deposited in a foreland basin during the Transamazonian Orogeny related to continent-continent collision to the east-southeast (Bertrand and Jardim de Sa, 1990; Machado and others 1996; Alkmim and Marshak, 1998). Sabará Group also contains thin poorly laminated lenticular beds of iron formation and ferruginous quartz arenite.

After deposition, the Minas Supergroup was subjected to two tectonic events, the Transamazonian (ca. 2.2 - 2.0 Ga) and Brasiliano (ca. 0.6 - 0.5 Ga) orogenies (Marshak and Alkmim, 1989). The first event affected the whole area while the second affected only the eastern part of the Quadrilátero Ferrífero and produced west-verging fold-and-thrust system. The first event formed northwest-verging folds and thrusts during the convergence stage and dome-and-keel structures during the following extension (Marshak and others, 1992). The cumulative degree of regional metamorphism of the Minas Supergroup based on mineral assemblages is low-grade greenschist facies, either chlorite or biotite isograd (Herz, 1978).

DESCRIPTION OF SAMPLED SECTIONS

The Gandarela Formation was sampled in the type area at Gandarela Farm located in the center of the Gandarela syncline (fig. 3) about 40 kilometers southeast from Belo Horizonte. While the syncline is an allochtonous overturned structure (Chemale and others, 1994), the type area apparently experienced little deformation (Babinski and others, 1995). The Gandarela Formation is ~750 meters thick in this area (Dorr, 1969) and poorly exposed. Six partial sections were sampled on a meter to decimeter scale (fig. 4). Five of these are in the core of the Gandarela syncline and one (Loc. 5GND on fig. 3) is at the Extramil quarry where alternating red and buff dolomites of the Gandarela Formation are in stratigraphic contact with the Cauê Iron Formation. Carbonates above this level are buff colored argillaceous dolomite and dolomitic breccia followed by dolomites containing lenses of dolomitic iron formation (4GND), and then a thick sequence of alternating centimeter scale white and dark-gray banded limestones with occasional oolites (sections GA, GND, and 2GND). The basal part of

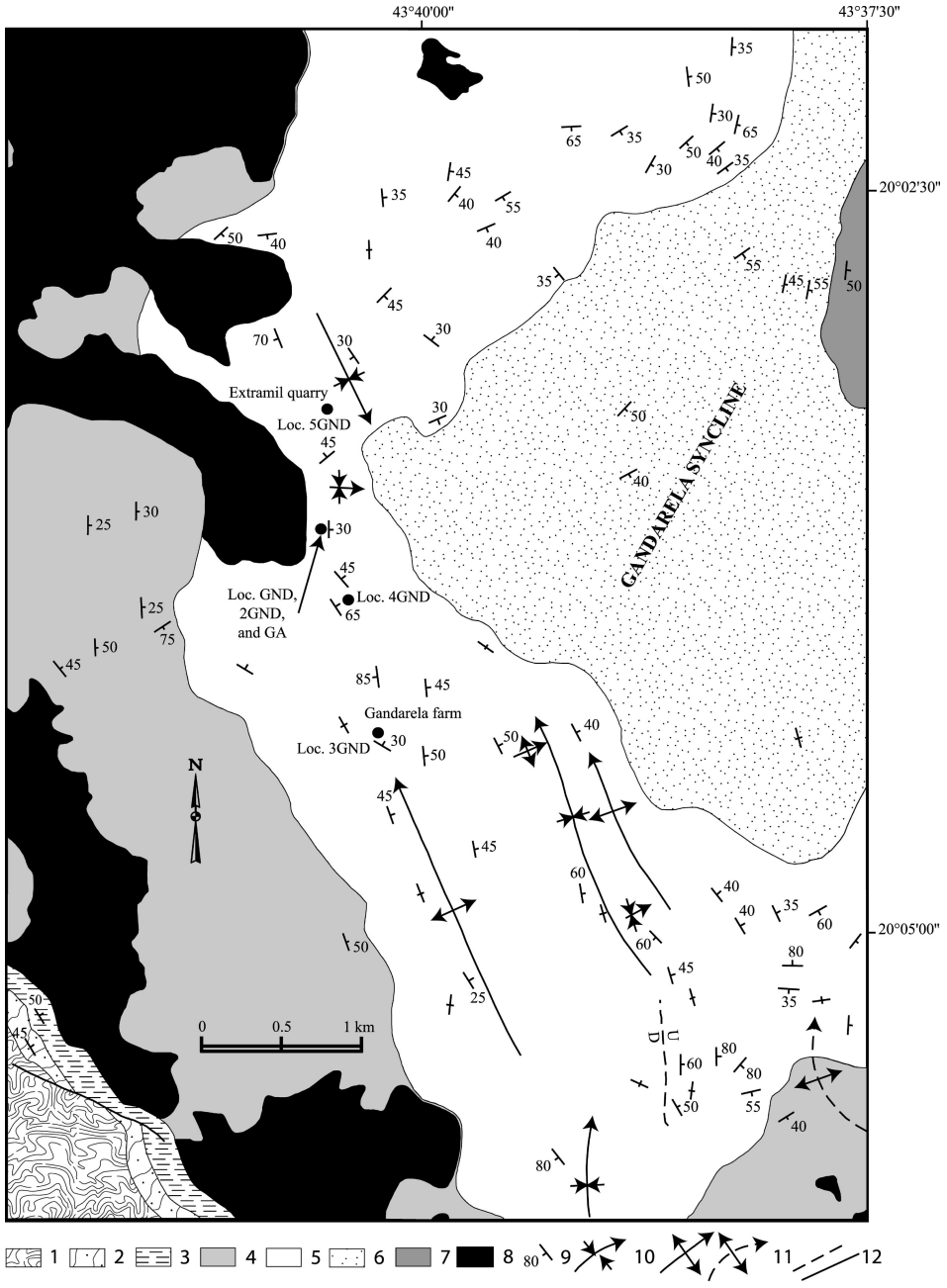

Fig. 3. Geological map of the Gandarela syncline (modified from Dorr, 1969) with localities where partial sections of the Gandarela Formation were sampled shown. 1 – Archean Nova Lima Group; 2 – Moeda Formation; 3 – Batatal Formation; 4 – Cauê Iron Formation; 5 – Gandarela Formation; 6 – Cercadinho Formation; 7 – Sabará Formation; 8 – Quaternary and Tertiary surficial and lake deposits; 9 – strike and dip; 10 – plunging syncline; 11 – plunging anticline, dashed where approximately located; 12 – fault, dashed where approximately located.

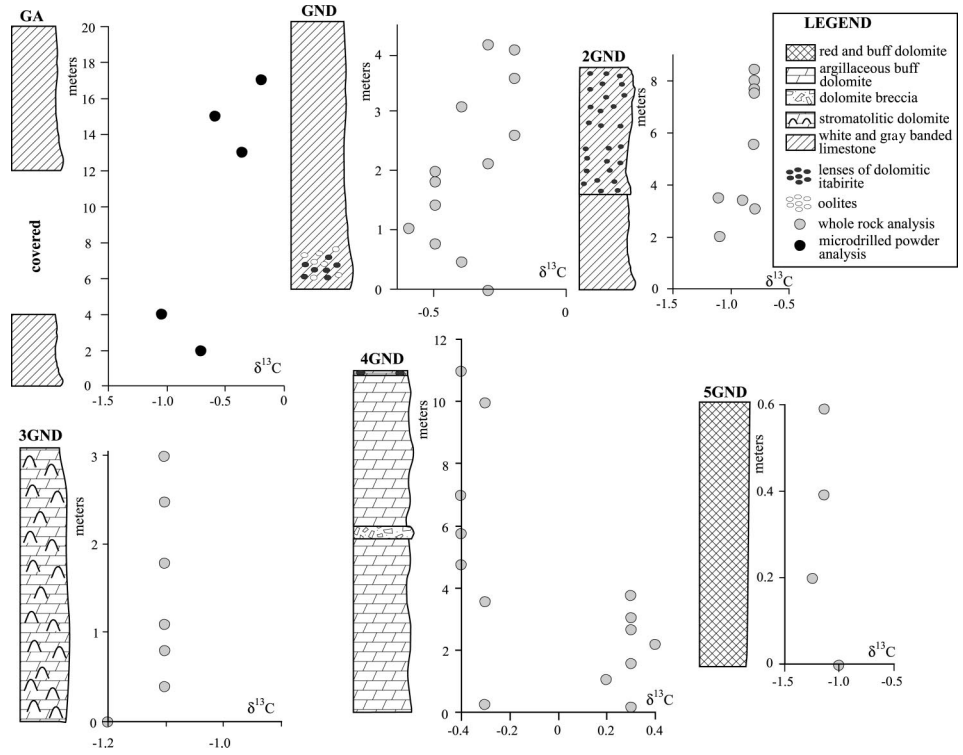

Fig. 4. Measured sections of the Gandarela Formation from the Gandarela syncline with $\delta^{13}C$ (‰ vs. PDB) values shown. Note that stratigraphic position of measured sections in respect to each other is uncertain due to poor outcrop and large distances between measured sections; see text for further discussion. Average $\delta^{13}C$ values were plotted for samples on which replicate whole rock analyses were run.

the GND section and the 2GND section contains lenses of dolomitic itabirite (=iron-formation). Oolites are present in the basal part of the GND section that sits stratigraphically several meters above the 2GND section. The GA section covers approximately both the GAND and 2GAND sections. The upper part of the Gandarela Formation is marked by stromatolitic dolomites (section 3GND).

A 45 meter thick carbonate section was also sampled at the Hargreaves quarry in the Dom Bosco syncline, about 40 kilometers southwest of Ouro Preto (fig. 1). This section represents the upper part of the Gandarela Formation, consisting of massive, argillaceous, and stromatolitic dolomites (fig. 5). In addition, carbonates of the upper Gandarela Formation were sampled in the Curral anticline (locality GA-20-1 on fig. 1).

Dolomite lenses of the Cercadinho Formation were sampled in the Curral anticline within the Sabará town in the eastern part of the Nova Lima Quadrangle (locality S on fig. 1) and 10 kilometers southwest from this locality along the strike (locality CE-20-1 on fig. 1). The section at locality CE-20-1 is near the base of the formation. An 11 meter thick carbonate lens within the steeply-dipping quartz arenite of the upper Cercadinho Formation (Gair, 1962) was sampled with high-resolution in locality S. The carbonate section starts with ferruginous dolomite that grade upward into pink and white dolomite (fig. 6).

Carbonates and phyllites of the Fecho do Funil Formation were sampled in the Cumbi quarry (20°27′49″S; 40°00′50″W) about 10 kilometers south of the town of Cachoeira do Campo in the north-central part of the Dom Bosco Quadrangle

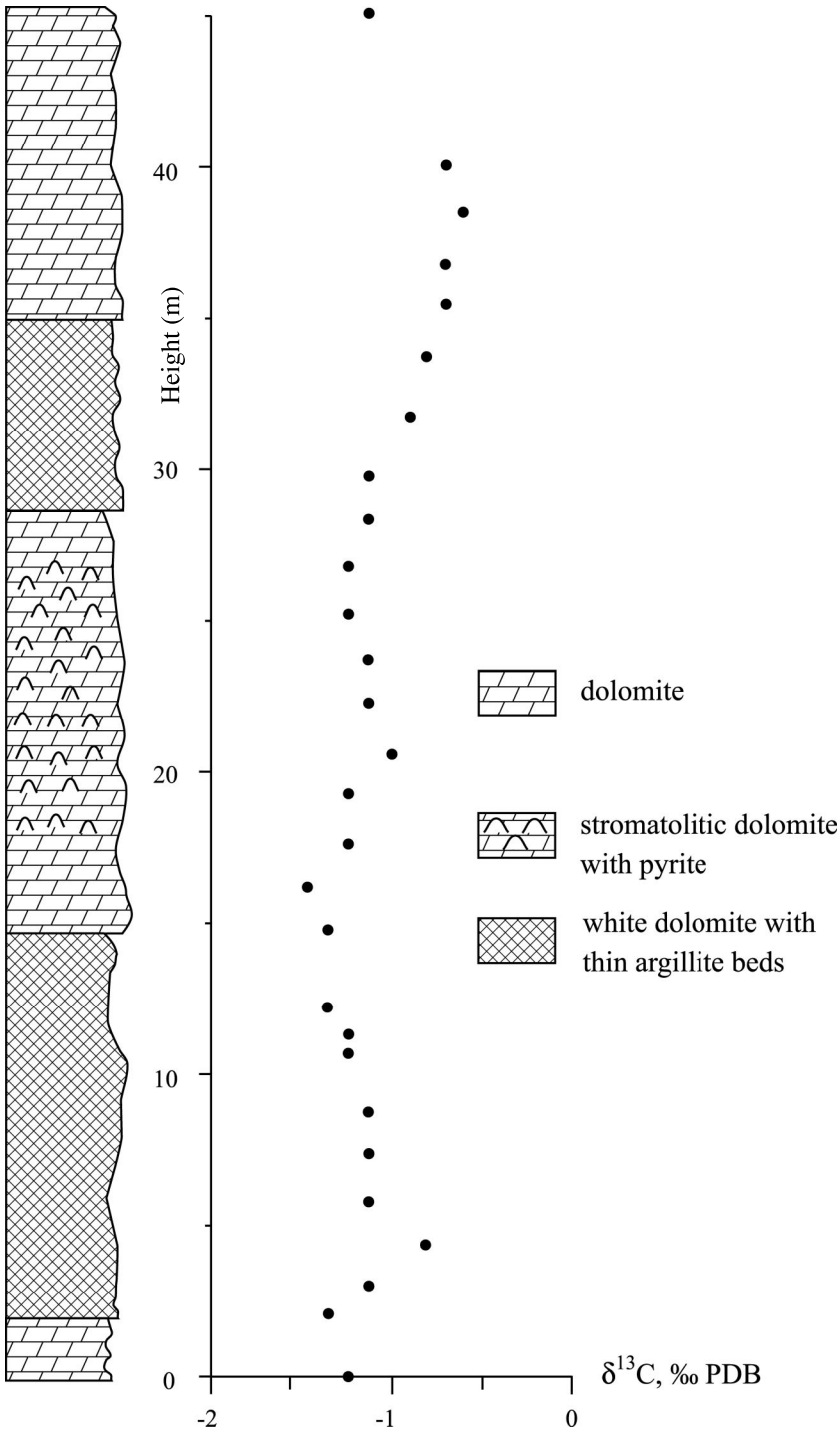

Fig. 5. Stratigraphic section of the Gandarela Formation in the Hargreaves quarry with $\delta^{13}C$ values of whole rock analysis shown.

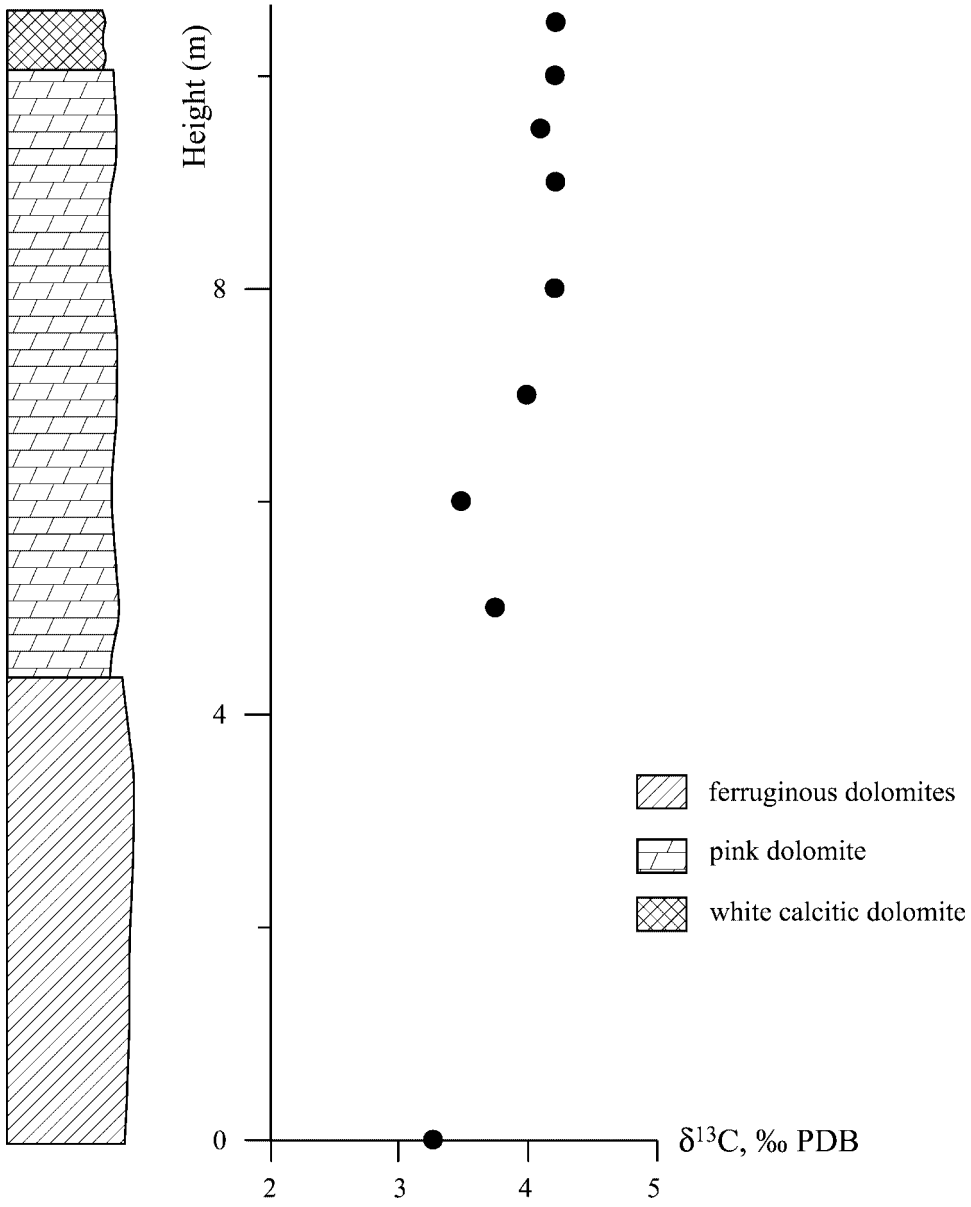

Fig. 6. Stratigraphic section of the 11m-thick dolomite lens in steeply-dipping quartz arenite of the upper Cercadinho Formation, Sabará town, eastern part of the Nova Lima Quadrangle with $\delta^{13}C$ values of whole rock analysis shown.

(Johnson, 1962). Dolomites form three lenses enclosed within carbonaceous, gray phyllites at the top of the formation and below carbonaceous phyllites of the Barreiro Formation. Two large lenses, which are over 100 meters long and up to 50 meters thick, were sampled (fig. 7). Carbonate samples previously analyzed in the Pb-Pb study (MSF-series; Babinski and others, 1995) collected in the same quarry were also analyzed for carbon and oxygen isotopes in this study. Dolomites are white, red, and

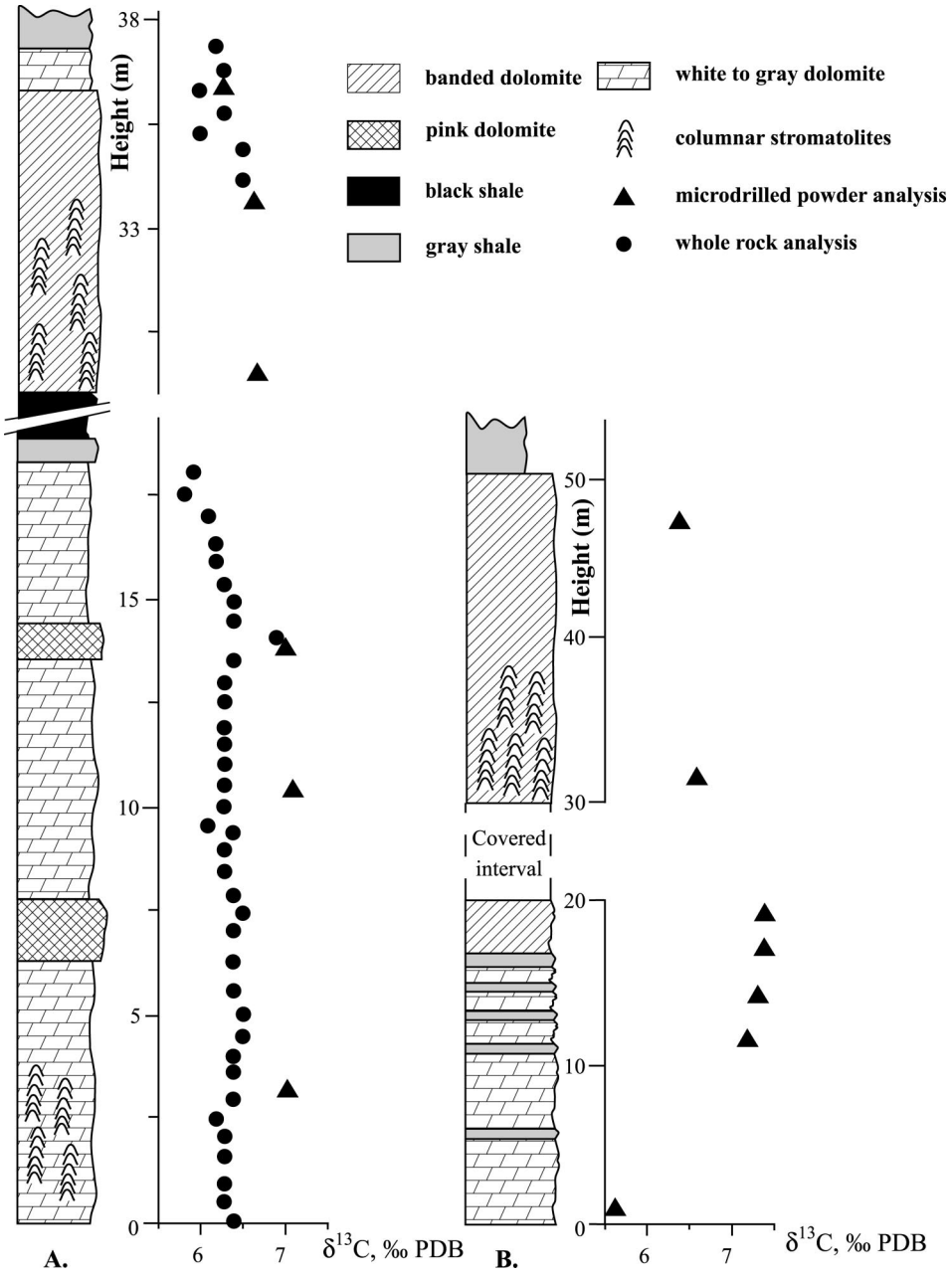

Fig. 7. Stratigraphic sections of dolomite lenses in the Fecho do Funil Formation, Cumbi quarry with $\delta^{13}C$ variations shown. A – northern wall section; B – southern wall section.

gray, massive and laminated, and contain carbonaceous phyllite and beds with columnar stromatolites and oncolites. The lower contact of the southern lens is not exposed and the upper part of this lens displays complex folding. The northern lens is fully exposed from the base to the top and the section is structurally undisturbed. Columnar

stromatolites are well preserved and common. The lens likely represents the upper half and the covered interval of the southern lens. Carbonaceous phyllites of the Barreiro Formation were also sampled in this locality. Finally, white and pink dolomites of the Fecho do Funil Formation were sampled in the Morro do Bule locality in the southern part of the Dom Bosco Quadrangle (Johnson, 1962; fig. 1).

ANALYTICAL METHODS

Carbonate sections were measured and samples were collected from thick stratigraphic intervals of pure carbonates without shear, foliation or fracture zones. Two sets of samples were independently collected for this study. One set of samples was cleaned, cut, and powdered for whole rock analyses. Least altered (that is lacking veins, discoloration, weathered rinds, recrystallization features, and silicification) and finest-grained portions of polished thick sections of the second set of samples were microdrilled with 1 millimeter diamond drills. Major and trace element concentrations in whole rock powders analyzed at the Geological Survey of Finland were determined by dissolution of ~10 milligrams of carbonate powder in 5 milliliters of 0.5 M acetic acid and subsequent analysis on ICP-AES (table 1). Microdrilled powders of ~20 to 40 milligrams were dissolved in 5 milliliters of 2 percent nitric acid and Mn and Sr contents were measured on a Buck Scientific 200-A AAS at Virginia Tech. Uncertainties based on the measurement of multiple standard materials by both methods were better than 5 percent for Sr and Fe and 10 percent for Mn. Major and trace element analyses at the LABISE, Federal University of Pernambuco were done by X-ray fluorescence, using fused beads and an automatic RIX-3000 (RIGAKU) unit. Fused beads were prepared using Li fluoride and Li tetraborate and uncertainties based on the measurement of multiple standard materials by this method were better than 5 percent for Sr and Fe and 10 percent for Mn.

Carbon dioxide was extracted at the Geological Survey of Finland from whole rock and microdrilled powders by closed tube reaction with anhydrous phosphoric acid ($\rho > 1.89$ g/cc) for 16+ hours at a temperature of 25°C for limestone and for one hour at 100°C for dolomite, and isolated by cryogenic distillation for mass spectrometric analysis on a Finnigan MAT 251. The fractionation factors used for mineral correction of oxygen isotopes in calcite prepared at 25°C (1.01025) and dolomite at 100°C (1.00913) were taken from Friedman and O'Neil (1977) and Rosenbaum and Sheppard (1986), respectively. The external precision based on multiple standard measurements of NBS-19 was better than 0.1 permil versus PDB for carbon and oxygen. Carbonate samples analyzed at the University of Maryland were microdrilled and the powders reacted with anhydrous phosphoric acid at 90°C in a Micromass MultiFlow head space analyzer. The resulting carbon dioxide was delivered to a Micromass IsoPrime mass spectrometer in a stream of high purity He. The reproducibility of carbon isotope compositions of standard materials by this technique were better than 0.1 permil, however, the system was not optimized for oxygen isotope analyses, and the uncertainty on these measurements are considerably larger (~1.3‰; n = 65). The fractionation factor used for mineral correction of oxygen isotopes in dolomite prepared at 90°C was 1.00932 (Rosenbaum and Sheppard, 1986). CO_2 gas from whole rock powders analyzed at the LABISE was extracted on a high vacuum line, after reaction with 100 percent phosphoric acid at 25°C for one day (three days for dolomite and calcite-dolomite mixtures), and cryogenically cleaned, according to the method described by McCrea (1950). Released CO_2 gas was analyzed in a dual inlet, triple collector VG Micromass SIRA mass spectrometer. The external precision based on multiple standard measurements of NBS-19 was better than 0.1 permil for carbon and oxygen.

TOC was isolated from powdered samples by repeated acidification and centrifugation with concentrated HCl followed by washing until the sample reached neutral

TABLE 1

Results of chemical and isotopic analyses. Analytical uncertainties are better than 10% for Mn, Fe and Sr, based on repeated analyses of standard materials. The external precision of isotopic measurements is better than 0.1‰ for both carbon and oxygen based on multiple analysis of the NBS-19 carbonate standard. Replicate analyses are marked with extensions A, B, and C.

Sample #	Height (m above the base)	TOC, mgC/g sample	$\delta^{13}C_{org}$ (‰, PDB)	$\delta^{13}C_{carb}$ (‰, PDB)	$\delta^{18}O_{carb}$ (‰, PDB)	$\Delta^{13}C_{carb\text{-}org}$	Analyzed mineral / rock	Fe, %	Mn, ppm	Sr, ppm	Mn/Sr	Rb, ppm	$^{87}Sr/^{86}Sr$
Gandarela Formation													
					a) Gandarela Farm								
GA-1+	13	0.03	-20.7	-0.4	-8.2	20.3	calcite		7627	286	26.7		
GA-2A+	15	0.06	-21.6	-0.6	-8.8	21.0	calcite		6869	524	13.1		
GA-2B+	15	0.08	-22.5	-0.5	-9.2	22.0	calcite		7614	495	15.4		
GA-3+	17	0.06	-18.7	-0.2	-9.3	18.5	calcite		4895	409	12.0		
GA-4+	2	0.08	-23.5	-1.0	-9.3	22.5	calcite		3224	430	7.5		
GA-5+	4	0.16	-24.5	-0.8	-9.7	23.7	calcite		2253	704	3.2		
5GND-1^	0			-1.0	-8.6		dolomite	1.28	15202	79	192.4	1	0.71124
5GND-2^	0.2			-1.2	-6.9		dolomite						
5GND-3^	0.4			-1.3	-6.4		dolomite						
5GND-4^	0.6			-1.3	-8.6		dolomite	0.51	11955	63	189.8	3	
4GND-1^	0.1			0.3	-7.1		dolomite	1.08	4898	64	76.5	2	
4GND-2^	0.2			-0.3	-6.5		dolomite						
4GND-3^	1.0			0.2	-7.9		dolomite						
4GND-4^	1.5			0.3	-6.7		dolomite						
4GND-5^	2.1			0.4	-6.2		dolomite						
4GND-6^	2.6			0.3	-6.5		dolomite						
4GND-7^	3.0			0.3	-6.5		dolomite	0.85	4209	19	221.5	0	
4GND-8^	3.5			-0.3	-6.4		dolomite						
4GND-9^	3.4			0.3	-7.0		dolomite						
4GND-10^	4.4			-0.4	-8.3		dolomite						

Table 1
(continued)

Sample #	Height (m above the base)	TOC, mgC/g sample	$\delta^{13}C_{org}$ (‰, PDB)	$\delta^{13}C_{carb}$ (‰, PDB)	$\delta^{18}O_{carb}$ (‰, PDB)	$\Delta^{13}C_{carb-org}$	Analyzed mineral / rock	Fe, %	Mn, ppm	Sr, ppm	Mn/Sr	Rb, ppm	$^{87}Sr/^{86}Sr$
4GND-11^	5.7			-0.4	-8.3		dolomite						
4GND-12^	6.9			-0.4	-8.2		dolomite						
4GND-13^	9.9			-0.3	-8.0		dolomite						
4GND-14^	10.9			-0.4	-8.4		dolomite						
GND-1^	0.5			-0.3	-8.5		calcite	0.46	7205	432	16.7	2	
GND-2^	0.8			-0.4	-8.7		calcite						
GND-3-A^	1.1			-0.5	-9.1		calcite						
GND-3-B^	1.1			-0.4	-7.5		calcite						
GND-4-A^	1.5			-0.6	-9.2		calcite	0.17	7169	432	16.6	4	
GND-4-B^	1.5			-0.5	-9.2		calcite	1.38	8022	560	14.3	2	
GND-5-A^	1.9			-0.6	-9.0		calcite	1.72	7523	523	14.4	1	
GND-5-B^	1.9			-0.4	-8.8		calcite						
GND-6-A^	2.1			-0.6	-8.7		calcite	0.12	6949	459	15.1	1	
GND-6-B^	2.1			-0.4	-9.0		calcite						
GND-7-A^	2.2			-0.4	-9.3		calcite						
GND-7-B^	2.2			-0.6	-8.8		calcite						
GND-8^	2.4			-0.3	-7.9		calcite	3.13	4990	663	7.5	4	
GND-9^	2.9			-0.2	-8.3		calcite						
GND-10-A^	3.4			-0.6	-8.6		calcite	0.52	5972	665	9.0	7	0.70339
GND-10-B^	3.4			-0.2	-7.2		calcite						
GND-11-A^	3.9			-0.2	-6.5		calcite						
GND-11-B^	3.9			-0.2	-7.4		calcite						
GND-12-A^	4.4			-0.2	-7.3		calcite	0.35	5664	607	9.3	2	

TABLE 1
(continued)

Sample #	Height (m above the base)	TOC, mgC/g sample	$\delta^{13}C_{org}$ (‰, PDB)	$\delta^{13}C_{carb}$ (‰, PDB)	$\delta^{18}O_{carb}$ (‰, PDB)	$\Delta^{13}C_{carb-org}$	Analyzed mineral / rock	Fe, %	Mn, ppm	Sr, ppm	Mn/Sr	Rb, ppm	$^{87}Sr/^{86}Sr$
GND-12-B^	4.4			-0.2	-6.8		calcite	3.69	6733	462	14.6	10	
GND-13^	4.5			-0.3	-8.5		calcite						
2GND-1^	2.0			-1.1	-9.2		calcite						
2GND-2^	3.0			-0.8	-9.6		calcite	3.09	2094	889	2.4	14	
2GND-3^	3.4			-0.9	-9.4		calcite						
2GND-4-A^	3.5			-1.6	-10.8		calcite	2.77	1608	977	1.6	16	
2GND-4-B^	3.5			-0.8	-9.2		calcite	1.20	6433	609	10.6	1	
2GND-4-C^	3.5			-0.8	-9.2		calcite						
2GND-5^	5.5			-0.8	-9.2		calcite						
2GND-6^	7.5			-0.8	-9.3		calcite	2.35	1959	895	2.2	10	
2GND-7-A^	7.6			-0.8	-9.3		calcite						
2GND-7-B^	7.6			-0.8	-9.0		calcite						
2GND-8^	8.0			-0.8	-9.4		calcite	2.99	2326	854	2.7	17	0.70416
2GND-9^	8.4			-0.8	-9.4		calcite						
3GND-1^	0.0			-1.2	-7.0		dolomite						
3GND-2^	0.4			-1.1	-6.0		dolomite	2.44	2900	82	35.4	14	0.71692
3GND-3^	0.8			-1.1	-6.1		dolomite						
3GND-4^	1.1			-1.1	-7.0		dolomite	2.62	2184	81	27.0	27	
3GND-5^	1.8			-1.1	-7.0		dolomite						
3GND-6^	2.5			-1.1	-6.0		dolomite						
3GND-7^	3.0			-1.1	-6.6		dolomite						
					b) Hargreaves quarry								
HARG 1^	0			-1.2	-10.1		dolomite	2.25	11046	64	172.6	12	

Table 1
(continued)

Sample #	Height (m above the base)	TOC, mgC/g sample	$\delta^{13}C_{org}$ (‰, PDB)	$\delta^{13}C_{carb}$ (‰, PDB)	$\delta^{18}O_{carb}$ (‰, PDB)	$\Delta^{13}C_{carb\text{-}org}$	Analyzed mineral / rock	Fe, %	Mn, ppm	Sr, ppm	Mn/Sr	Rb, ppm	$^{87}Sr/^{86}Sr$
HARG 2^	2			-1.3	-10.1		dolomite						
HARG 3^	3			-1.1	-9.9		dolomite	2.14	12331	63	195.7	13	
HARG 4^	4.5			-0.8	-9.3		dolomite						
HARG 5^	5.8			-1.1	-9.3		dolomite	2.85	15002	51	294.2	6	
HARG 6^	7.4			-1.1	-10.1		dolomite						
HARG 7^	8.8			-1.1	-10.1		dolomite	2.50	14619	87	168.0	29	
HARG 8^	10.7			-1.2	-10.6		dolomite						
HARG 9^	12			-1.2	-10.9		dolomite						
HARG 10^	11.3			-1.3	-11.1		dolomite	3.07	16339	87	187.8	9	
HARG 11^	14.7			-1.3	-11.0		dolomite						
HARG 12^	16.3			-1.4	-12.3		dolomite	3.15	15815	80	197.7	2	
HARG 13^	17.6			-1.2	-11.0		dolomite						
HARG 14^	19.2			-1.2	-12.1		dolomite						
HARG 15^	20.5			-1.0	-13.5		dolomite	2.74	14824	110	134.8	2	
HARG 16^	22.2			-1.1	-10.2		dolomite						
HARG 17^	23.8			-1.1	-11.8		dolomite						
HARG 18^	25.3			-1.2	-10.8		dolomite	2.80	1817	103	17.6	6	
HARG 19^	26.8			-1.2	-10.2		dolomite						
HARG 20^	28.3			-1.1	-10.1		dolomite	3.51	15880	57	278.6	0	
HARG 21^	29.8			-1.1	-9.9		dolomite						
HARG 22^	31.8			-0.9	-8.7		dolomite						
HARG 23^	33.6			-0.8	-8.9		dolomite	1.36	11470	42	273.1	2	
HARG 24^	35.3			-0.7	-8.7		dolomite						

TABLE 1
(continued)

Sample #	Height (m above the base)	TOC, mgC/g sample	$\delta^{13}C_{org}$ (‰, PDB)	$\delta^{13}C_{carb}$ (‰, PDB)	$\delta^{18}O_{carb}$ (‰, PDB)	$\Delta^{13}C_{carb-org}$	Analyzed mineral / rock	Fe, %	Mn, ppm	Sr, ppm	Mn/Sr	Rb, ppm	$^{87}Sr/^{86}Sr$
HARG 25^	36.9			-0.7	-9.0		dolomite	1.48	11427	56	204.1	0	
HARG 26^	38.5			-0.6	-8.2		dolomite						
HARG 27^	40.1			-0.7	-9.0		dolomite						
HARG 28^	45.1			-1.1	-10.4		dolomite						
				c) Locality GA-20/1 in Curral anticline									
GA-20/1#		0.06		-0.9	-10.1		dolomite		1896	22	87.4		
Cercadinho Formation													
				a) Locality CE-20-1 in Curral anticline									
CE-20/1#		0.08	-16.4	5.4	-9.6	21.8	dolomite		279	21	13.4		
				b) Sabará town									
SAB-1^	0.0			3.3	-9.9		dolomite	9.22	1992	36	55.3	8	
SAB-2^	5.0			3.8	-9.7		dolomite	1.15	897	69	13.0	9	
SAB-3^	6.0			3.5	-8.9		dolomite	4.82	886	41	21.6	17	
SAB-4^	7.0			4.0	-8.5		dolomite	2.28	772	44	17.5	5	
SAB-5^	8.0			4.2	-8.6		dolomite	1.03	760	48	15.8	10	
SAB-6^	9.0			4.2	-8.1		dolomite	1.03	618	44	14.0	6	
SAB-7^	9.5			4.1	-8.0		dolomite	0.85	675	40	16.9	16	
SAB-8^	10.0			4.2	-8.0		dolomite						
SAB-9^	10.5			4.2	-8.3		dolomite	0.86	806	42	19.2	10	
CE-20/2#				3.7	-9.3		dolomite		631	16	39.2		
Fecho do Funil Formation													
				a) Cumbi quarry									
Southern lens, heights of samples above the basal contact													
PC-1+	0	0.06	-19.7	5.6	-12.2	25.3	dolomite		1820	60	30.2		

Table 1
(continued)

Sample #	Height (m above the base)	TOC, mgC/g sample	$\delta^{13}C_{org}$ (‰, PDB)	$\delta^{13}C_{carb}$ (‰, PDB)	$\delta^{18}O_{carb}$ (‰, PDB)	$\Delta^{13}C_{carb\text{-}org}$	Analyzed mineral / rock	Fe, %	Mn, ppm	Sr, ppm	Mn/Sr	Rb, ppm	$^{87}Sr/^{86}Sr$
PC-2+	12	0.08	-14.4	7.2	-12.3	21.6	dolomite		3242	35	93.0		
PC-3+	15		-24.8	7.3	-11.6	32.1	dolomite		2046	17	123.0		
PC-4+	17.5	0.09	-23.5	7.4	-11.0	30.9	dolomite		2249	20	115.4		
PC-5+	20	0.07	-21.9	7.4	-11.0	29.3	dolomite		1583	26	61.3		
PC-6+	32	0.04	-19.7	6.6	-10.6	26.3	dolomite		1153	11	107.0		
PC-7+	47.5	0.08	-15.2	6.4	-10.9	21.6	dolomite		1272	13	101.6		
PC-8+	50	0.06	-18.7				shale						
Northern lens, heights of samples above the basal contact													
PC-15+	3.0	0.07	-19.0	7.0	-10.6	26.0	dolomite		1213	21	56.7		
PC-16+	10.3	0.11		7.1	-10.6		dolomite		1285	6	200.6		
PC-17+	13.8	0.07	-20.7	7.0	-10.9	27.7	dolomite		1118	5	228.6		
PC-18+	29.7	0.10	-24.4	6.7	-10.9	31.1	dolomite		1094	5	221.4		
PC-19+	33.7	0.08	-23.4	6.6	-11.0	30.0	dolomite		1291	12	105.9		
PC-20+	36.4	0.07	-22.7	6.3	-11.2	29.0	dolomite		1425	11	124.4		
PC-21+	39.1	0.18	-24.7				Shale						
CUMBI 1^	0			6.4	-9.8		dolomite	0.99	1185	43	27.6	41	
CUMBI 2^	0.5			6.3	-9.8		dolomite						
CUMBI 3^	1.0			6.3	-10.6		dolomite						
CUMBI 4^	1.5			6.3	-10.0		dolomite						
CUMBI 5^	2.0			6.3	-9.7		dolomite	0.63	1124	48	23.4	98	0.71137
CUMBI 7^	2.5			6.2	-10.4		dolomite						
CUMBI 8^	3.0			6.4	-10.3		dolomite						
CUMBI 9^	3.5			6.4	-10.0		dolomite						
CUMBI 10^	4.0			6.4	-9.7		dolomite	0.55	1366	47	29.1	14	

Table 1
(continued)

Sample #	Height (m above the base)	TOC, mgC/g sample	$\delta^{13}C_{org}$ (‰, PDB)	$\delta^{13}C_{carb}$ (‰, PDB)	$\delta^{18}O_{carb}$ (‰, PDB)	$\Delta^{13}C_{carb-org}$	Analyzed mineral / rock	Fe, %	Mn, ppm	Sr, ppm	Mn/Sr	Rb, ppm	$^{87}Sr/^{86}Sr$
CUMBI 11^	4.5			6.5	-9.5		dolomite						
CUMBI 12^	5.0			6.5	-10.7		dolomite	0.67	1394	45	31.0	17	0.70302
CUMBI 14^	5.5			6.4	-9.5		dolomite						
CUMBI 15a^	6.0			6.4	-9.5		dolomite	0.65	1500	61	24.6	11	
CUMBI 15b^	6.5			6.4	-9.4		dolomite						
CUMBI 16^	7.0			6.5	-9.4		dolomite						
CUMBI 17^	7.5			6.4	-9.5		dolomite						
CUMBI 18^	8.0			6.3	-9.5		dolomite						
CUMBI 19^	8.5			6.3	-9.5		dolomite						
CUMBI 20^	9.0			6.4	-9.6		dolomite	0.58	1401	48	29.2	19	
CUMBI 21^	9.5			6.1	-9.9		dolomite						
CUMBI 22^	10.0			6.3	-9.7		dolomite						
CUMBI 23^	10.5			6.3	-9.6		dolomite						
CUMBI 24^	11.0			6.3	-9.8		dolomite						
CUMBI 25^	11.5			6.3	-9.7		dolomite	0.57	1272	53	24.0	15	
CUMBI 26^	12.0			6.3	-9.7		dolomite	0.65	1330	51	26.1	15	
CUMBI 27^	12.5			6.3	-9.7		dolomite						
CUMBI 28^	13.0			6.3	-9.7		dolomite						
CUMBI 29^	13.5			6.4	-9.7		dolomite						
CUMBI 30^	14.0			6.9	-9.6		dolomite	0.41	1142	53	21.5	18	0.72282
CUMBI 31^	14.5			6.4	-9.7		dolomite						
CUMBI 32^	15.0			6.4	-9.8		dolomite						
CUMBI 33^	15.5			6.3	-9.8		dolomite						

Table 1
(continued)

Sample #	Height (m above the base)	TOC, mgC/g sample	$\delta^{13}C_{org}$ (‰, PDB)	$\delta^{13}C_{carb}$ (‰, PDB)	$\delta^{18}O_{carb}$ (‰, PDB)	$\Delta^{13}C_{carb\text{-}org}$	Analyzed mineral / rock	Fe, %	Mn, ppm	Sr, ppm	Mn/Sr	Rb, ppm	$^{87}Sr/^{86}Sr$
CUMBI 34^	16.0			6.2	-10.0		dolomite						
CUMBI 35^	16.5			6.2	-10.0		dolomite	0.86	1563	84	18.6	15	
CUMBI 36^	17.0			6.1	-10.0		dolomite						
CUMBI 37^	17.5			5.8	-10.4		dolomite						
CUMBI 38^	18.0			5.9	-10.7		dolomite						
CUMBI 41^	34.0			6.5	-10.6		dolomite	1.23	2065	98	21.1	27	
CUMBI 42^	34.5			6.5	-10.6		dolomite	0.78	2136	111	19.2	16	
CUMBI 43^	35.0			6.0	-10.7		dolomite	5.47	926	57	16.2	87	
CUMBI 44^	35.5			6.3	-10.3		dolomite						
CUMBI 45^	36.0			6.0	-11.0		dolomite	5.01	1465	69	21.2	84	
CUMBI 46^	36.5			6.3	-10.7		dolomite	4.72	1537	72	21.3	59	
CUMBI 47^	37.0			6.2	-10.8		dolomite	5.87	1004	50	20.1	93	
MF-1-A*				6.7	-10.9		dolomite	0.42	1214	56	21.7		
MF-1-B*				6.7	-10.9		dolomite	0.50	1196	56	21.5		
MF-1-C*				6.6	-10.8		dolomite	0.46	1405	50	27.9		
MF-1-D*				6.7	-10.9		dolomite	0.55	1249	59	21.3		
MF-1-E*				6.7	-10.8		dolomite	0.54	1331	52	25.7		
MF-1-F*				6.6	-10.8		dolomite	0.38	1348	48	27.9		
MF-1-G*				6.7	-10.8		dolomite	0.28	1221	49	24.9		

TABLE 1
(continued)

Sample #	Height (m above the base)	TOC, mgC/g sample	$\delta^{13}C_{org}$ (‰, PDB)	$\delta^{13}C_{carb}$ (‰, PDB)	$\delta^{18}O_{carb}$ (‰, PDB)	$\Delta^{13}C_{carb-org}$	Analyzed mineral / rock	Fe, %	Mn, ppm	Sr, ppm	Mn/Sr	Rb, ppm	$^{87}Sr/^{86}Sr$
MF-1-H*				6.7	-10.7		dolomite	0.30	1285	48	27.0		
MF-1-I*				6.7	-10.8		dolomite	0.26	1286	48	27.1		
					Morro do Bule locality								
FUNIL-1^				6.4	-9.4		dolomite	0.81	1410	47	30.0	9	
FUNIL-2^				6.4	-9.5		dolomite	0.93	1346	46	29.3	12	
FUNIL-3^				7.1	-9.1		dolomite	0.81	1297	51	25.4	14	
Barreiro Formation (Cumbi quarry)													
PC-22*		17.8	-26.6				Shale						

* C and O isotope values, and major and trace element concentrations were measured at the Geological Survey of Finland.
+ C and O isotope values of carbonates were measured at the Geological Survey of Finland; TOC content was measured at the University of Maryland; carbon isotope values of organic carbon were measured at the Mountain Mass Spectrometry; trace element contents were measured at VPI & SU.
# C and O isotope values of carbonates and TOC content were measured at the University of Maryland; carbon isotope values of organic carbon were measured at the Mountain Mass Spectrometry; trace element contents were measured at VPI & SU.
^ C and O isotope values and major and trace element concentrations in carbonates were measured at the NEG-LABISE; Sr isotope work was done at the Institute of Geosciences, UnB, Brasilia.

pH (Kaufman and Knoll, 1995). Dried samples in Vycor tubes were then mixed with CuO, evacuated, sealed and combusted at 850°C for 12 hours. The volume of CO_2 quantified during cryogenic distillation was used to calculate the TOC content. The carbon isotope composition in extracted and purified CO_2 was measured with a VG PRISM mass spectrometer at Mountain Mass Spectrometry and with a Finnigan MAT 251 at the Geological Survey of Finland. To test for the uncertainty of abundance and isotopic composition measurements on TOC, replicate (n = 4) analyses of organic-rich and organic-poor powders were run in the previous study (Bekker and others, 2001a). For analyses of the organic-rich sample, uncertainties were ± 0.26 mgC/g for abundance (5.57 mgC/g average) and ± 0.03 permil for carbon isotopic composition (-34.47‰ average). For the organic-poor sample uncertainties were ± 0.06 mgC/g (0.18 mgC/g average) and ± 1.3 permil (-24.1‰ average) for abundances and carbon isotopic compositions, respectively. Blanks analyzed in this study contained 0.74 and 1.02 μmoles of CO_2 and had carbon isotope values of -20.28 and -20.27 permil, respectively.

Samples chosen for Sr isotopic analyses were leached in 0.5 M acetic acid and centrifuged to separate the dissolved and insoluble fractions. Sr was eluted from solutions by ion exchange chromatography using Sr-Spec resin. $^{87}Sr/^{86}Sr$ values were determined in static mode using a Finnigan MAT 262 seven-collector mass spectrometer at the University of Brasília, Brazil. The isotopic ratios were normalized to $^{86}Sr/^{88}Sr$ value of 0.1194 and the 2σ uncertainties on Sr isotope measurements was less than 0.00009. Repeated analyses of NBS-SRM 987 standard with a ratio of 0.710140 given by NBS over the analysis period indicated a value of 0.71024 +/- 0.00007 (2σ) for the $^{87}Sr/^{86}Sr$ ratio.

EVALUATING SAMPLE QUALITY

Diagenesis and metamorphism can affect the isotopic composition of sedimentary carbonates. Therefore, validity of measured C, O and Sr isotopic ratios as synsedimentary values reflecting seawater composition need to be verified by screening samples through a battery of geochemical and petrographic tests.

Oxygen isotopes are known to be sensitive indicators of alteration, with marked decrease in $\delta^{18}O$ values often resulting from isotopic exchange with meteoric or hydrothermal fluids. It has been estimated that in diagenetic environments three orders of magnitude higher water-rock ratios are required to alter carbon isotope values compared to those of oxygen isotope values (Banner and Hanson, 1990). During metamorphism, relative shifts of $\delta^{13}C$ versus those of $\delta^{18}O$ will depend on many parameters including whether it is an open or closed system, whether equilibrium with coexisting silicates was reached or not, T, and CO_2/H_2O ratios (Baumgartner and Valley, 2001). For example, while batch volatization causes moderate change in $\delta^{13}C$, Rayleigh volatization leads to a much more pronounced decrease in $\delta^{13}C$, while $\delta^{18}O$ values do not show significant difference between these two cases (Valley, 1986). Cross-plots of $\delta^{13}C$ values versus $\delta^{18}O$ values may show whether carbon isotope values were strongly affected by alteration based on presence or lack of correlation between these two parameters. While oxygen isotope composition of the Paleoproterozoic seawater is poorly constrained, $\delta^{18}O$ values ranging from -6 to –12 permil are common to the least altered Paleoproterozoic carbonate successions (for example Burdett and others, 1990; Veizer and others, 1992a, 1992b; Melezhik and others, 1997b; Bekker and others, 2001a, 2003).

Meteoric alteration has been shown to increase Mn and Fe contents in carbonates while decreasing their Sr content, resulting in the widespread use of Mn/Sr or Fe/Sr as an index of alteration (Kaufman and Knoll, 1995). However, Archean and early Paleoproterozoic carbonates, especially dolomites, are known to contain more Fe and Mn than Phanerozoic or Neoproterozoic carbonates (Veizer and others, 1989a, 1989b,

1990, 1992a, 1992b), complicating the application of the Mn/Sr ratio as an index of alteration. Nonetheless, within a single basin elemental ratios still provide a relative basis for comparison of the diagenetic alteration of closely spaced samples belonging to the same depositional setting. Samples with high Rb content, commonly localized in clays, are inappropriate for Sr isotope work since ^{87}Rb decay would alter primary Sr isotope values.

Dolomites are abundant in Precambrian carbonate successions yet their synsedimentary versus diagenetic origin remains debatable. Since dolomites generally contain less Sr than calcites and could have formed in equilibrium with fluids ranging in composition from seawater to deep burial waters, they are generally considered less likely to preserve primary C, O, or Sr isotope signals. However, we found in previous studies and in this study that dolomites as well preserve $\delta^{13}C$ signature as limestones and appear to have generally higher O isotope values (Bekker and others, 2001a, 2003). In addition, some Paleoproterozoic dolomites with relatively low Sr contents appear to preserve near to primary Sr isotope values (Master and others, 1990; Gorokhov and others, 1998; Bekker and others, 2003). Good preservation of depositional carbon isotope compositions in Paleoproterozoic dolomites is thus likely related to synsedimentary or early diagenetic dolomitization in the presence of seawater solutions.

Maturation of organic matter generally results in the ^{13}C enrichment of the residual organic carbon (Hayes and others, 1983), whereas alteration of inorganic carbon generally results in lower $\delta^{13}C$ values. Consequently, difference between isotopic composition of organic and carbonate carbon ($\Delta^{13}C_{carb\text{-}org}$) decreases with the degree of alteration. Depositional $\Delta^{13}C_{carb\text{-}org}$ values depend on a number of environmental factors including p_{CO_2}, type of organic matter, and growth rate. For the last 800 Ma average measured $\Delta^{13}C_{carb\text{-}org}$ value is roughly 30 permil, ranging from modern values of less than 28 permil to Neoproterozoic extremes of greater than 32 permil (Hayes and others, 1999). Unless environmental conditions resulted in strong carbon limitation (Popp and others, 1998; Bigidare and others, 1999), significantly smaller $\Delta^{13}C_{carb\text{-}org}$ values are likely to reflect a higher degree of alteration or metamorphism.

While all the petrographic and geochemical screens are open to debate, the greatest confidence in the preservation of primary isotopic trends comes from the consistency of the curves based on closely-spaced samples collected in sequence stratigraphic framework from multiple sections within the depositional basin. Correlating trends from separate basins worldwide is clearly more difficult, and requires that detailed studies be conducted in all of them.

GEOCHEMICAL DATA AND DIAGENESIS

Carbonates in this study from all three formations have experienced greenschist facies metamorphism, but were sampled in areas of low strain and far from intrusions. Thin sections (n = 21) were prepared for samples that were microdrilled (see table 1). The thin sections were stained with Alizarin Red S and potassium ferricyanide to identify calcite, Fe-rich dolomite and Fe-poor dolomite. These samples contain xenotopic mosaic of anhedral coarsely-crystalline to very coarsely-crystalline grains of either dolomite or calcite (compare Gregg and Sibley, 1984) with pseudospar and veins and fractures filled with quartz, very coarsely-crystalline carbonate and muscovite. Blue staining indicating Fe-rich dolomite is lacking in most thin sections and when it is present, it covers much less than 1 percent of a thin section and marks small (<15 μm in size) crystals. While micrite and microspar did not survive through neomorphism and recrystallization during diagenesis and low grade metamorphism, gross primary textures (for example laminations) remain. Following Dorr (1969) we refer to these

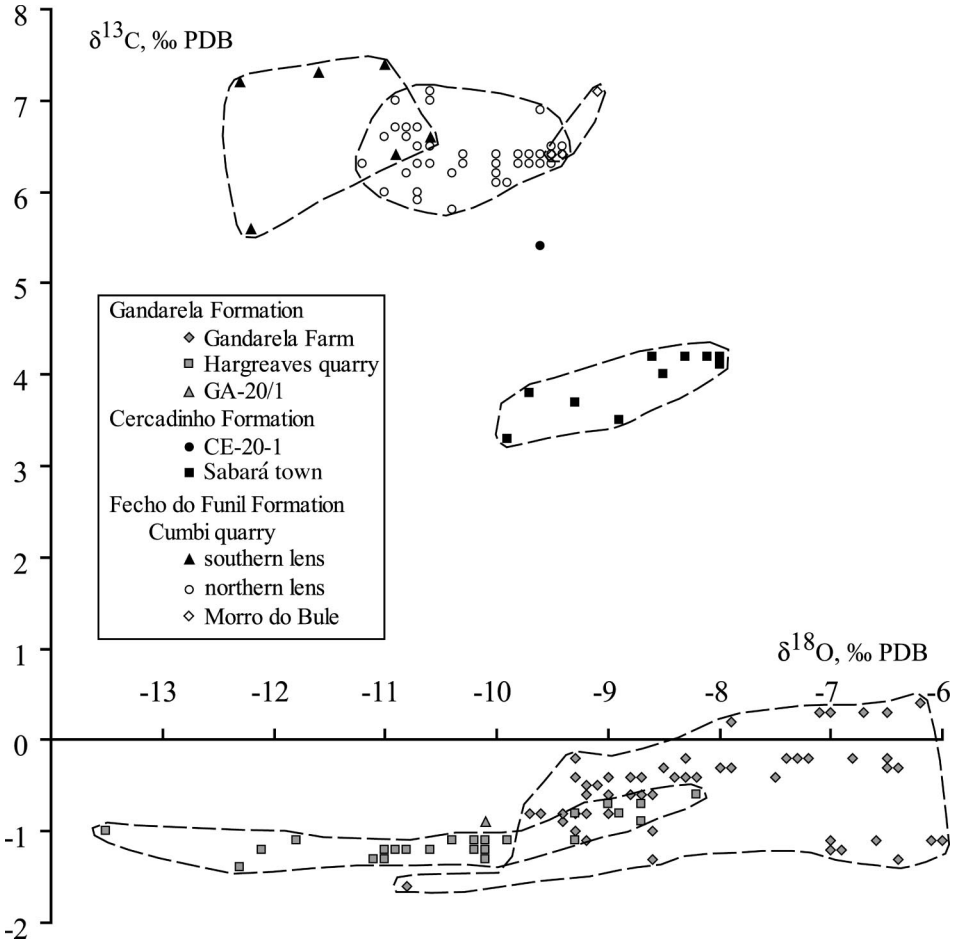

Fig. 8. Scatter diagram of $\delta^{13}C$ values versus $\delta^{18}O$ values for studied carbonates. Dashed lines highlight fields of values for carbonates from different units and localities.

carbonate rocks as dolomite and limestone, although based on their position in the metamorphic sequence and their grain size we imply crystalline dolomite and calcite.

The Gandarela Formation

Geochemical analyses are provided in table 1. Most samples are dolomite except for limestone in the GA-, GND-, and 2GND- series. Samples have highly variable, but uncorrelated $\delta^{18}O$ values (-13.5 to -6.0‰) and Mn (1,608 – 16,339 ppm), Fe (0.12 – 3.69%), and Sr (19 – 977 ppm) contents. Limestones have higher Sr content (286 – 977 ppm) than dolomites suggesting an aragonite precursor (compare Veizer, 1983). Isotopic and elemental variations are controlled by primary and diagenetic signals specific to locality and stratigraphic position. For example, carbonates from the Gandarela syncline have higher $\delta^{18}O$ values than those from Hargreaves quarry and Curral anticline (fig. 8) suggesting better preservation. Dolomites from Hargreaves quarry also have unusually high Fe and Mn contents with only dolomites from the basal part of the Gandarela Formation at the Gandarela farm having comparable Mn contents. On average, dolomites have higher $\delta^{18}O$ values than limestones in the

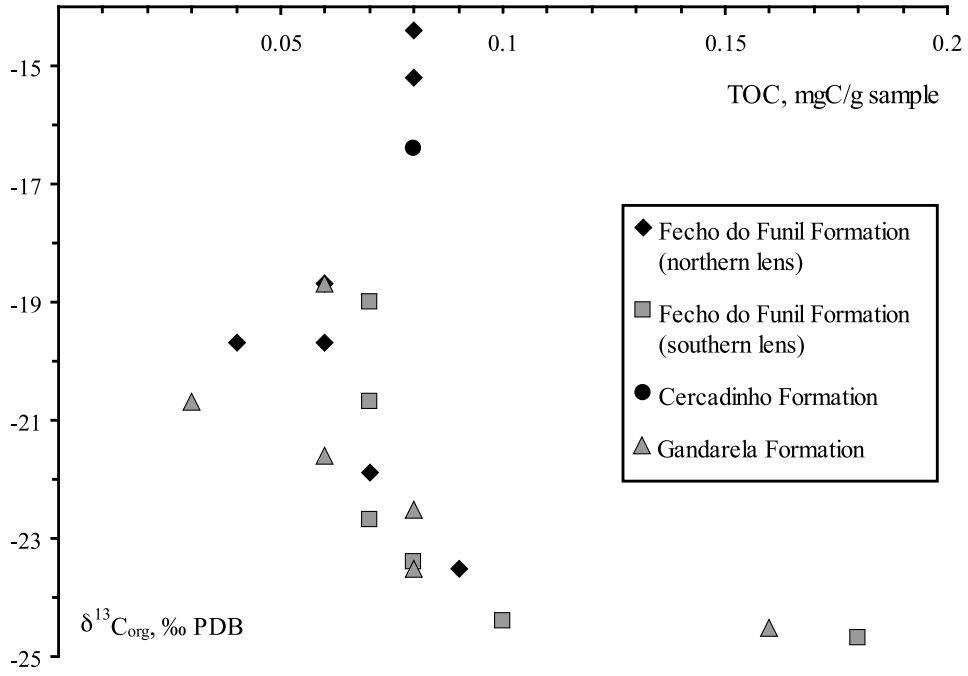

Fig. 9. Scatter plot of $\delta^{13}C_{org}$ values vs. TOC content for studied units (Barreiro data are not included). Note large range of $\delta^{13}C_{org}$ values for samples with TOC content less than 0.1 mgC/g sample.

Gandarela syncline, while carbon isotope values in both rocks are essentially identical. Most samples have $\delta^{18}O$ values above -10.5 permil consistent with those found in well-preserved Paleoproterozoic carbonate successions. $\Delta^{13}C_{carb\text{-}org}$ values are small, ranging from 18.6 to 23.8 permil, as are TOC contents (0.03 – 0.16 mgC/g sample; fig. 9). $\delta^{13}C$ values vary between -1.6 and +0.4 permil (figs. 4 and 5). Red dolomite, at the base of the formation in the 5GND section (fig. 4), displays the most negative $\delta^{13}C$ values ranging from -1 to -1.3 permil. Four limestone samples with high Sr content were analyzed for Sr isotope ratios. The lowest measured $^{87}Sr/^{86}Sr$ value was 0.70339.

The Cercadinho Formation

The eleven analyzed dolomite samples (table 1) have highly variable Mn (279-1,992 ppm), Fe (0.85 – 9.22 %), and Sr (16 – 69 ppm) contents, but a rather narrow range of $\delta^{18}O$ values (-9.9 to -8.0‰). Carbon isotope values from the Sabará section range from +3.3 to +5.4 permil and smoothly increase up-section (fig. 6). Oxygen isotope values show a similar trend in this section. The sample SAB-1, at the base of the section, was likely strongly altered as it has unusually high Mn and Fe contents and the lowest oxygen and carbon isotope values and Sr content. Iron and manganese contents marginally co-vary with $\delta^{13}C$ values, but other variables do not appear to be related. The source of these co-variations and the lack of those between $\delta^{18}O$ and either Mn or Fe is not understood but might reflect seawater stratification in respect to Mn and Fe contents and carbon isotope values rather than post-depositional alteration.

The Fecho do Funil and Barreiro Formations

Seventy-two dolomite and shale samples of the Fecho do Funil and Barreiro formations were analyzed (table 1). Dolomites had highly variable Mn (926 – 3,242

ppm), Fe (0.26 – 5.87 %) and Sr (5 – 111 ppm) contents. Oxygen isotope values range from -12.3 to -9.1 permil and most samples have $\delta^{18}O$ values above –11 permil. Shales and carbonates of the Fecho do Funil Formation have highly variable $\delta^{13}C_{org}$ values, ranging from -24.8 to -14.4 permil, and low TOC contents (0.04 – 0.18 mgC/g sample). Samples with TOC content less than 0.1 mgC/g sample have higher $\delta^{13}C$ values suggesting limited exchange between organic carbon and carbonate (fig. 9). $\Delta^{13}C_{carb\text{-}org}$ values range from 21.6 to 32.1 permil, with the highest values suggesting good preservation for carbon isotope values of carbonate and organic carbon. In contrast, shale of the Barreiro Formation has much higher TOC content (17.8 mgC/g sample) and $\delta^{13}C_{org}$ value of -26.6 permil, which is within the range of values found in shales and dolomites of the underlying Fecho do Funil Formation. $\delta^{13}C$ values of dolomites range from +5.6 to +7.4 permil but reveal no clear stratigraphic trend (fig. 7). Isotopic values (fig. 8) and elemental abundances do not appear to correlate. Sample Cumbi-12 yielded the lowest Sr isotope ratio of 0.70302 for the Fecho do Funil and the Minas Supergroup. The 0.70302 value is similar to the lowest Sr isotope values (0.7030 – 0.7035) measured in correlative ^{13}C-enriched carbonates of Fennoscandia and Zimbabwe (Master and others, 1990; Gorokhov and others, 1998; fig. 10).

Interpretation of Carbon Isotope Data

Carbon isotope data of the Gandarela Formation are similar to those found in all studied marine carbonates older than ca. 2.32 Ga (Veizer and others, 1989a, 1989b, 1990, 1992a, 1992b) supporting the interpretation based on a number of diagenetic screens that they reflect seawater composition slightly modified by diagenetic and metamorphic alteration. Carbon isotope values of the Cercadinho and Fecho do Funil formations are highly ^{13}C-enriched and outside of the $\delta^{13}C$ range of typical marine carbonate. Therefore, local processes that might produce ^{13}C-enrichment need to be considered before inferring global seawater composition from these data. High organic carbon burial in lacustrine or closed basin (compare Schidlowski and others, 1976b; Botz and others, 1988) can be excluded based on an open-marine setting inferred from sedimentologic data. Both evaporation in shallow-water settings (Stiller and others, 1985) and methanogenesis in organic-rich sediments (Irwin and others, 1977) can produce dolomites with high $\delta^{13}C$ values. While the Cercadinho Formation was deposited in a shallow-marine setting, no evidence for evaporites are known. The Fecho do Funil Formation was deposited in a deep-water setting outside of the likely influence of evaporation. Methanogenesis can significantly increase carbon isotope values of bicarbonate below the sediment-water interface (Claypool and Kaplan, 1974). Diagenetic and burial dolomite produced under this influence has highly positive carbon isotope values reaching up to +27 permil (Friedman and Murata, 1979; Talbot and Kelts, 1986) and occurs as crystals, concretions, laminae, and thin discontinuous beds within organic-rich sediments with TOC content $\geq$1 percent. These dolomites have highly variable carbon isotope values even within a single crystal or concretion (Hennessy and Knauth, 1985; Winter and Knauth, 1992a). Difference in $\delta^{13}C$ values as large as 10 permil is common between stratigraphically or laterally proximal samples (Friedman and Murata, 1979; Hennessy and Knauth, 1985). Early carbonate lithification and large carbon reservoir precludes significant effect of methanogenesis on carbon isotope composition of organic-rich carbonate successions. This effect has not been documented on recent or Phanerozoic carbonate platforms. The only possible exception are lithified carbonate frameworks (Sansone and others, 1990) which are absent on early Precambrian carbonate platforms.

Effects of methanogenesis on carbon isotope values of early Precambrian carbonates are poorly documented with only two examples described (Winter and Knauth, 1992b; Dix and others, 1995). Winter and Knauth (1992b) studied carbonate nodules from ca. 1.88 Ga organic-rich shales of the Rove Formation, Ontairo, Canada. They

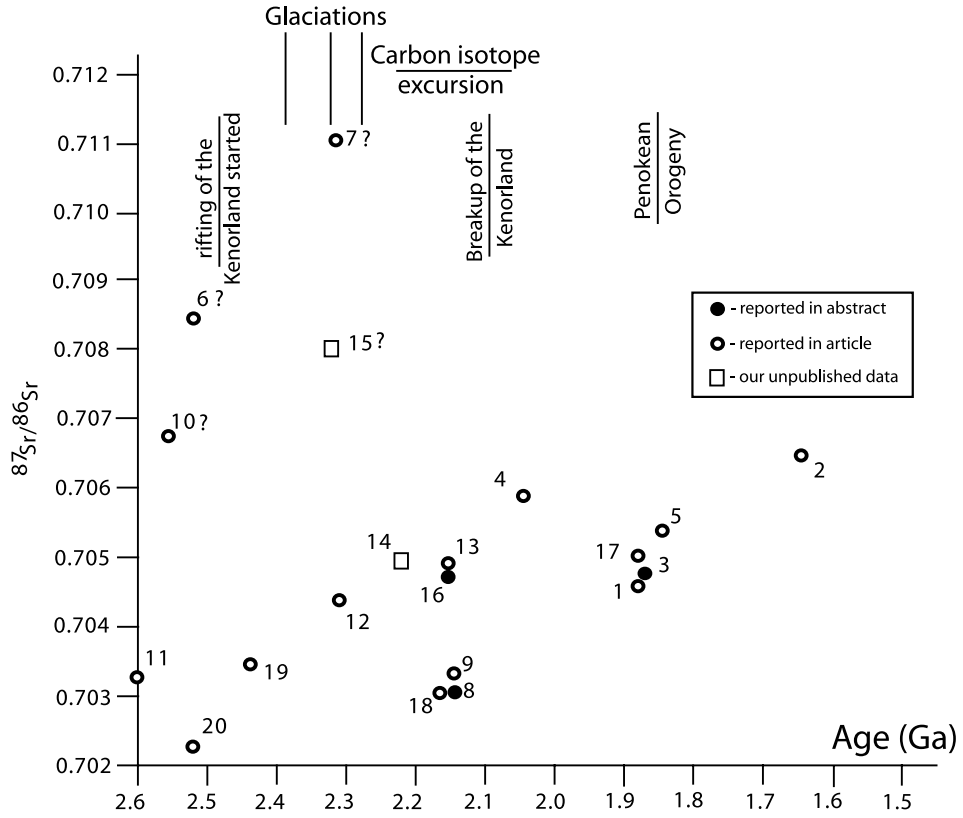

Fig. 10. Sr isotope values of the Paleoproterozoic carbonates compiled from literature with additional data from this study. 1 - Coronation Supergroup, Wopmay Orogen; 2 - McArthur Group, Australia; 3 - Gunflint Formation, Ontario; 4 - upper part of the Lower Albanel Formation, Quebec; 5 - Duck Creek Dolomite, Australia; 6 - Malmani Subgroup, South Africa; 7 - Espanola Formation, Ontario; 8 - Lomagundi Group, Zimbabwe; 9 - Tulomozero Formation, Russia; 10 - Wittenoom Formation, Australia; 11 - Carawine Dolomite, Australia; 12 - Duitschland Formation, Chuniespoort Group, South Africa; 13 - Nash Fork Formation, WY; 14 – Kona Dolomite, MI; 15 - Vagner Formation, WY; 16 - Alder Formation, Knob Lake Group, Labrador Trough; 17 - Utsingi Formation, Pethei Group, Canada; 18 - Fecho do Funil Formation, Minas Group, Brazil (this paper); 19 - Gandarela Formation, Minas Group, Brazil (this paper); 20 - Gamohaan Formation, Campbellrand Subgroup, South Africa. References to the age constraints: 1 – Bowring and Grotzinger, 1992; 2 – Page and Sweet, 1998; 3 – Fralick and others, 2002; 4 - the final stage of the ca. 2.2 – 2.1 Ga carbon isotope excursion (Bekker and others, 1997); 5 – Pidgeon and Horwitz, 1991; 6 – Sumner and Bowring, 1996, Martin and others, 1998; 7 – sandwiched between the second and third glacial events; 8 – Schidlowski and Todt, 1998; 9 – Vasil'eva and others, 2000; 10 – Trendall and others, 1998; 11 – Nelson and others, 1999; 12 – sandwiched between the second and third glacial events (Bekker and others, 2001a); 13 – the final stage of the ca. 2.2 – 2.1 Ga carbon isotope excursion (Bekker and others, 2003); 14 – beginning of the ca. 2.2 – 2.1 Ga carbon isotope excursion (Bekker and Karhu, 1997; 15 – sandwiched between second and third glacial events; 16 – Rohon and others, 1993; 17 - Bowring and Grotzinger, 1992; 18, 19 – see Regional geology and stratigraphy section in this paper; 20 – Sumner and Bowring, 1996. References to Sr isotope data: 1, 2 – Veizer and others, 1992a; 3 – Faure and Powell, 1972; 4 – Mirota and Veizer, 1994; 5, 6, 7 – Veizer and others, 1992; 8 – Master and others, 1990; 9 – Gorokhov and others, 1998; 10, 11 – Veizer and others, 1990; 12 – Bekker and others, 2001a; 13 – Bekker and others, 2003; 14, 15 – Bekker and others, unpublished data; 16 – Kuznetsov and others, 2003; 17 – Whittaker and others, 1998; 18, 19 – this paper; 20 – Kamber and Webb, 2001. Units marked with the question mark have Sr isotope ratios outside of the likely range for the early Precambrian seawater.

found that within a single nodule carbon and oxygen isotope values of carbonate sampled from the core to the margin show a similar trend to the one in carbonate nodules formed by organic matter degradation in organic-rich sediments that passed

through the zones of sulfate reduction, methanogenesis, and thermal decarboxylation (Claypool and Kaplan, 1974). However, they did not find highly positive $\delta^{13}C$ values typical to methanogenesis. Dix and others (1995) documented $\delta^{13}C$ values as high as +14.5 permil PDB in dolomites of the Ribeirão das Antas Formation of the Crixás Greenstone Belt, Brazil. The succession experienced amphibolite grade metamorphism and Fe-rich dolomite form stratiform lenses and pods up to 50 meters thick within graphitic metapelite. Dix and others (1995) found Fe-poor diagenetic crystals and concretions within Fe-rich metamorphic dolomite. Both Fe-rich and Fe-poor dolomites have a similar range of oxygen and carbon isotope values. Dix and others (1995) suggested that Fe-poor dolomite was formed during early diagenesis within organic-rich marine carbonate lenses and inherited $\delta^{13}C$ values from bicarbonate derived by organic matter degradation during methanogenesis. Fe-rich dolomites were interpreted as recrystallized mixture of normal marine and diagenetic carbonates. However, since both types of dolomite have similar isotopic signature an alternative interpretation is possible. Fe-poor dolomite could have formed during early diagenesis in a rock-dominated system within marine Mg-rich calcite with high $\delta^{13}C$ values. During metamorphism, calcite was recrystallized into Fe-rich dolomite, while some remnants of early diagenetic dolomite survived. The latter model implies that highly positive carbon isotope values record seawater composition modified by diagenesis and metamorphism. The former model does not take into account the flux of methanogenically derived carbon necessary to produce 50 meter thick carbonate lens. Seawater composition of these carbonates is supported by recent studies of carbonates from the Crixás and correlative belts within the Goiás Massif, Brazil that indicate regional rather than local signature for this anomaly (Fortes and Jost, 1996; Fortes personal communication, 2003). Metasedimentary rocks of the Crixás greenstone belt have T_{DM} model ages mostly between 2.34 and 2.5 Ga and have structural contact with the underlying lower Archean mafic and ultramafic units (Fortes and others, 2003). Therefore, correlation between the Crixás carbonates and the ca. 2.2 – 2.1 Ga ^{13}C-enriched carbonates (Karhu and Holland, 1996) is warranted.

Could methanogenesis be responsible for ^{13}C-enriched signature of the Cercadinho and Fecho do Funil carbonates? Organic-rich rocks are lacking in the Minas Supergroup immediately below the Fecho do Funil and Cercadinho formations and phyllites interlayered with and inclosing carbonate lenses of the Fecho do Funil Formation are not organic-rich (see table 1). Low TOC content can not be explained by organic matter degradation since refractory organic carbon compounds are not consumed by methanogens and survive low metamorphic grade. $\delta^{13}C_{org}$ values are not consistent with significant contribution of methanotrophs to TOC and therefore do not provide support for oxidative methane cycling (compare Hayes, 1994). Carbon isotope values do not show large range and have consistent stratigraphic trend (note that whole rock and microdrilled powders were obtained from different sets of samples and 1‰ variations in $\delta^{13}C$ values between whole rock and microdrilled analyses are expected; Kaufman and others, 1991). Furthermore, Cercadinho and Fecho do Funil formations were sampled in two locations, yet carbon isotope values are consistent. We therefore infer that carbonates of the Fecho do Funil and Cercadinho formations reflect composition of the ocean.

Implications for the Evolution of the Early Paleoproterozoic Surface Environment

Heaman (1997) recognized the global extent of a 2.48 to 2.45 Ga tectonomagmatic event and related it to a mantle plume initiating protracted rifting of the Kenorland supercontinent. This event is recorded by thick mafic volcanics and associated BIFs in open-marine succession of Western Australia (Barley and others, 1997) and South Africa (ash beds in thick and extensive BIFs; see Pickard, 2003 for review of geochronol-

ogy). In Brazil, volcanism associated with this event is lacking, however the Cauê Iron Formation, which is somewhat older than 2.42 Ga (based on Pb-Pb carbonate age of the Gandarela Formation), might also have been deposited in response to this event. Geological evidence for Paleoproterozoic ice ages in the Minas Supergroup of Brazil is also lacking; we propose below that this glaciogenic interval is lost along the unconformity between the Gandarela and Cercadinho formations. In this view, the compressional event that led to the unconformity in Brazil might be time equivalent with the initiation of a foreland basin in Western Australia, which was filled with predominantly siliciclastic deposits of the Turee Creek Group (Krapež, 1996), and with the compressional event that folded units underlying the glacially-influenced Makganyene and Rooihoogte formations in South Africa (Altermann and Hälbich, 1991; Bekker and others, 2001a; fig. 11). This event has not been dated in Brazil with the exception of model ages of Pb isotope resetting in galenas from Archean deposits (Thorpe and others, 1984). Consequently, it is possible that the Gandarela Formation postdates the tectonomagmatic event and possibly predates the beginning of the glacial epoch, which followed the tectonomagmatic event in North America (Young and others, 2001).

Correlations between early Paleoproterozoic sedimentary successions of Brazil, South Africa, and Australia, supported by available radiometric ages, chemostratigraphy, and time-specific rock types are proposed in figure 11. Figure 12 illustrates how geochronology and chemostratigraphy of studied units fit with published curves of secular carbon isotope variations in the Paleoproterozoic. Based on presence of an angular unconformity below the Duitschland Formation and lack of similar hiatus in the Turee Creek Group as well as different carbon isotope signature of carbonates of the Turee Creek Group and the Duitschland Formation, we propose a correlation between the second of three glacial events of the Huronian Supergroup, Canada and the diamictite at the base of the Duitschland Formation (compare Bekker and others, 2001a); furthermore we tentatively correlate diamictite of the Meteorite Bore Member with the first glacial event of the Huronian Supergroup. Based on this compilation, the Gandarela Formation is roughly correlative with the Tongwane Formation, South Africa and the lower part of the Turee Creek Group, Australia. Carbonates of the Gandarela Formation and the Turee Creek Group in the Duck Creek syncline have carbon isotope values close to 0 permil (Bekker and others, 2002), while those from the Tongwane Formation have moderately ^{13}C-enriched values up to +3.5 permil (Bekker and others, 2001a). Carbonates of the Tongwane Formation are confined to a small area and they have not been studied in sufficient detail to warrant that these values represent the global signal. The Tongwane Formation is separated by a major unconformity from the overlying glacially-influenced Duitschland Formation (Bekker and others, 2001a). Combined, these data do not suggest that the carbon isotope composition of seawater prior to the early Paleoproterozoic glacial epoch was marked by significant and long-lasted ^{13}C-enrichment, as has been recorded in carbonates deposited *before* all Neoproterozoic ice ages and at least one Paleoproterozoic glaciation (Kaufman and others, 1997; Bekker and others, 2001a). It remains possible that evidence for the positive carbon isotope excursion preceding the glacial epoch is missing due to glacial erosion and the limited carbon isotope data. However, geological evidence for the rise of the atmospheric oxygen level, a likely consequence of carbon isotope excursion, is interpreted by us to appear only after the second glacial event (Bekker and others, 2001a). Based on the available $\delta^{13}C$ data, it seems unlikely that the glacial epoch was initiated by drawdown of atmospheric CO_2 associated with high relative burial rates of organic matter. The hypothesis that the early Paleoproterozoic climate change was initiated by methane oxidation (Pavlov and others, 2000) is also not supported by the available carbonate and organic carbon data, since they do

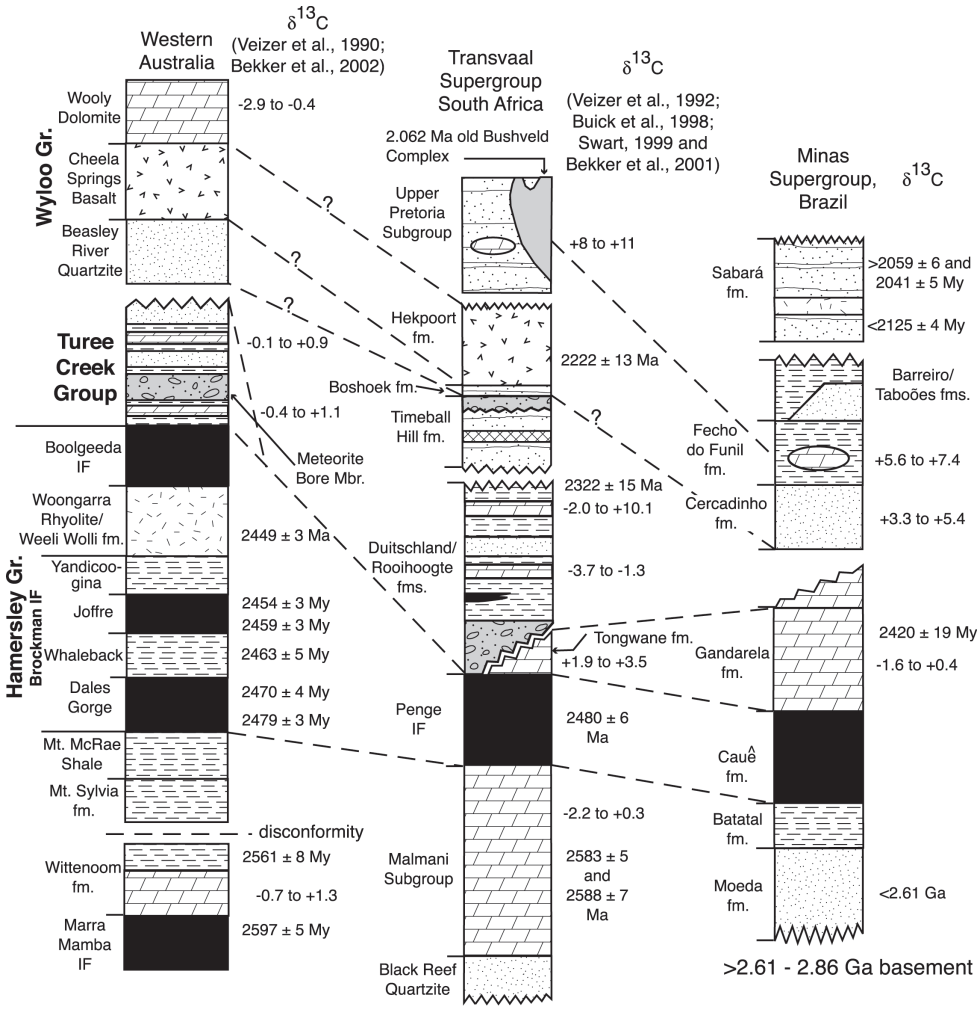

Fig. 11. Correlation between the Minas and Transvaal supergroups of Brazil and South Africa and Hamersley, Turee Creek and Wyloo groups of Western Australia. Only ca. 2.6 to 2.0 Ga old portions of these successions are shown. Correlations are based on chemostratigraphic data (published and presented in this paper), available geochronologic data and time-specific rock types (glacial diamictites, BIFs, and mature quartz arenites). Geochronological data for Brazil, South Africa and Western Australia were reviewed in the Regional geology and stratigraphy section of this paper; Nelson and others, 1999; Bekker and others, 2001a; Pickard, 2002 except for the Re-Os pyrite age of the Rooihoogte Formation, which is from Hannah and others, 2003. Mature quartzites occur in the Beasley River Quartzite, Western Australia; the Boshoek Formation (immediately above the glacial diamictite of the Timeball Hill Formation; Coetzee, ms, 2001) and the Dwaalheuvel Formation of the Upper Pretoria Subgroup (immediately above the Hekpoort Formation), South Africa; and in the Cercadinho Formation, Brazil. Note: the Turee Creek Group stratigraphy combines sections from the Hardey and Duck Creek synclines following Krapež (1996). Sawtooth pattern stands for unconformity.

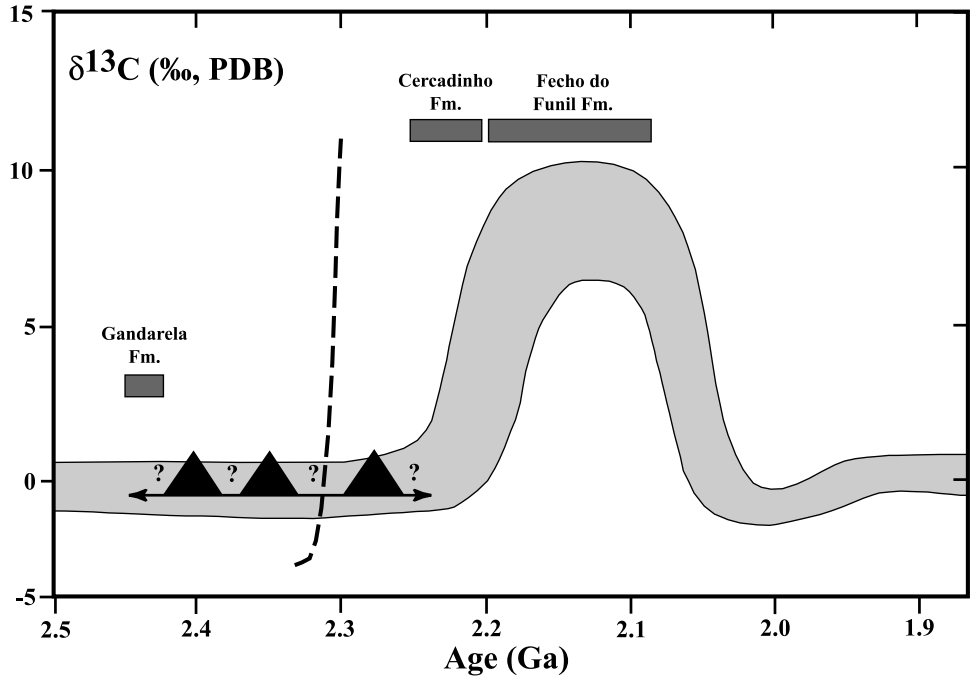

Fig. 12. Schematic representation of Paleoproterozoic $\delta^{13}C$ variations. Gray curve is after Karhu and Holland, 1996 with additional information shown in dashed line from Bekker and others, 2001a. Dashed line is based on the recently recognized positive carbon isotope excursion in the Duitschland Formation and the negative carbon isotope excursion in cap carbonates above the middle of three glacial diamictites in the Huronian and Snowy Pass supergroups and at the base of the Duitschland Formation (Veizer and others, 1992; Bekker and Karhu, 1996; Bekker and others, 1999, 2001a). Black triangles and question marks between them represent three Paleoproterozoic glacial events in North America and their age uncertainty. Depositional ages of studied units based on their geologic, geochronologic and chemostratigraphic (this paper) age constraints are shown.

not show negative carbon isotope anomalies beneath the first glacial event, which might be expected if significant amounts of methane were present and were oxidized (compare Hayes, 1994; Dickens and others, 1997; Jahren and others, 2001).

The youngest Paleoproterozoic glacial diamictite in North America and Fennoscandia is overlain by thick extremely mature hematitic quartzites and Al-rich shales (Young, 1973; Ojakangas, 1988). Hematitic mature quartzites and Al-rich shales were recently recognized in a similar stratigraphic position in respect to glacial deposits in South Africa (Dwaalheuwel Formation and Mapedi Shale/Lucknow Formation; Bekker and others, 2001a) providing further support for the global extent of these rock types in post-glacial successions. Some of these mature quartzites are intruded by 2.22 Ga mafic dikes and sills (for example in Fennoscandia and the Lorrain Formation of the Huronian Supergroup in Canada) while others overlie 2.22 Ga mafic volcanics (South Africa) and in all cases they underlie ca. 2.2 to 2.1 Ga old highly ^{13}C-enriched carbonates. The Cercadinho Formation, which contains mature, ferruginous quartz arenites and Al-rich shales and underlies ^{13}C-enriched carbonates of the Fecho do Funil Formation, likely correlates to these units deposited during the post-glacial climatic amelioration (fig. 11).

In the aftermath of the Paleoproterozoic glacial epoch, an increase in riverine P flux from landmasses experiencing intense weathering for the first time in contact with an oxidizing atmosphere could have increased productivity and thereby resulted in the

>2.22 to 2.1 Ga carbon isotope excursion. Carbon isotope values of thin carbonates associated with mature quartzites overlying the ultimate glacial horizon (Randville Dolomite, Marquette Range Supergroup, Michigan, USA; Lower Jatulian Group, Russia; Magusa and Whiterock members of the Kinga Formation, Hurwitz Group, Canada) are moderately ^{13}C-enriched (Yudovich and others, 1990; Tikhomirova and Makarikhin, 1993; Bekker and Karhu, 1997; Bekker and others, unpublished data), suggesting slight increase in the relative burial rate of organic matter. Carbonates of the Cercadinho Formation have similar carbon isotope values providing additional support that this unit was deposited shortly after the end of the glacial epoch.

Carbonates of the Fecho do Funil Formation have high δ^{13}C values similar to those found in carbonates deposited between ca. 2.22 and 2.1 Ga worldwide (Karhu and Holland, 1996). This correlation is supported by the match of remarkably low $^{87}Sr/^{86}Sr$ values (ca. 0.703) in these units (fig. 10). While ^{13}C-enriched carbonates are lacking above the Turee Creek Group in the Hamersley Basin, Western Australia, due to a major hiatus at the top of this group (Krapež, 1996), carbonates from the Silverton Formation of the Pretoria Group (Buick and others, 1998; Swart, ms, 1999) and the correlative Lucknow Formation of the Olifantshoek Group, South Africa (Swart, ms, 1999) and the Lomagundi and Deweras groups of Zimbabwe (Schidlowski and others, 1975, 1976a; Bekker and others, 2001b) are ^{13}C-enriched and likely broadly correlative with the Fecho do Funil Formation (fig. 11). Carbonates of the Ribeirão das Antas Formation of the Crixás Greenstone Belt, Brazil (Dix and others, 1995; Fortes and Jost, 1996) and ca. 2074 to 2145 Ma Paso Severino Formation, San Jose Belt, Uruguay (Bekker and others, 2003) have highly positive δ^{13}C values and are also broadly correlative with the Fecho do Funil Formation. Graphitic shales of the Barreiro Formation might reflect tectonic subsidence on the early stage of the foreland basin development related to the ca. 2.1 Ga Transamazonian orogeny.

It seems possible that enhanced silicate weathering associated with Kenorland rifting might have contributed to climate change and initiation of the glacial epoch through CO_2 drawdown. However, the low $^{87}Sr/^{86}Sr$ values of the pre-glacial Gandarela Formation (ca. 0.7034) are in conflict with this interpretation. This conflict may be resolved if the exposed and weathered mafic volcanic rocks extruded during the 2.48 to 2.45 Ga tectonomagmatic event delivered non-radiogenic Sr to seawater (Taylor and Lasaga, 1999; Bartley and others, 2001). Clearly high-resolution time series Sr isotope compositions of seawater through this critical interval are needed. From the available data, it appears that seawater Sr isotope ratios gradually increased between 2.6 and 1.6 Ga (fig. 10). This observation suggests that the transition in the ocean composition at the Archean-Proterozoic boundary from the mantle-buffered ocean to the one reflecting interplay between crustal and hydrothermal (mantle) fluxes (Veizer, 1994) must have continued for more than 1 Ga.

CONCLUSIONS

a) Carbonates of the Gandarela Formation provide carbon isotope data relevant to the seawater composition at ca. 2.4 Ga and arguably before the Paleoproterozoic glacial epoch. Combined with available data, our analyses from Brazil suggest that the δ^{13}C of seawater before the first Paleoproterozoic glacial event was close to 0 permil, and not highly ^{13}C enriched, and do not support hypotheses that the Paleoproterozoic glacial epoch was launched by either high relative burial rate of organic carbon or by methane oxidation. As an alternative, we propose that enhanced weathering due to rifting of the supercontinent positioned in low to middle latitude and associated compressional events on its margins contributed to climactic changes. The Cauê Iron Formation is likely correlative with BIFs in South Africa and Western Australia and might also be related to the 2.48 to 2.45 Ga tectonomagmatic event.

b) The Cercadinho Formation, at the base of the Piracicaba Group, was likely deposited shortly after the end of the glacial epoch and contains ferruginous mature quartz arenites and Al-rich shales with lenses of carbonates that have $\delta^{13}C$ values ranging from +3.3 to +5.4 permil. These data add to the growing body of evidence that the Paleoproterozoic glacial epoch was superceded by a dramatic climatic amelioration exposing continents to the CO_2- and oxygen-rich atmosphere. Seawater composition immediately after the end of the glacial epoch was slightly ^{13}C-enriched but did not reach the level of ^{13}C-enrichment typical for the following ca. 2.22 to 2.1 Ga carbon isotope excursion. This slight ^{13}C-enrichment in carbonates deposited shortly after the end of the glacial epoch either belongs to the rising limb of the following carbon isotope excursion or represents short-term perturbations in the seawater composition preceding the ca. 2.22 to 2.1 Ga carbon isotope excursion.

c) Dolomites of the Fecho do Funil Formation record the global ca. 2.22 to 2.1 Ga carbon isotope excursion in Brazil and are correlative with the Paleoproterozoic ^{13}C-enriched carbonates worldwide.

ACKNOWLEDGMENTS

Field and laboratory work was supported by the CNPq projects n. 461984/00-8 and 463029/00-3 granted, respectively to ANS and VPF. Thanks are due to G. M. Santana and V. S. Bezerra for the assistance with carbon and oxygen isotope analyses at the NEG-LABISE and to I. S. Barbosa for XRF analyses in the Federal University of Pernambuco, Brazil. S. D. S. Barros and N. C. Guerra helped with figure drafting. Simone Gioia is thanked for technical assistance in the geochronology laboratory at the University of Brasília. This is the contribution n. 193 of the NEG-LABISE. M. Babinski and W. R. Van Schmus provided samples used in their geochronologic work that stimulated our further work. D. Rimstidt provided access to and helped with AAS work. Support for AB came from GSA and southeastern section of GSA; Colorado Scientific Society; and the graduate school and Department of Geological Sciences, VPI and SU. JAK thanks the Geological Survey of Finland for permission to publish data produced in their laboratories and A. Henttinen for assistance. Funding for participation by AJK and isotopic analyses at the University of Maryland was provided by NSF grants EAR-98-17348 and EAR-0126378 and NASA Exobiology grant NAG 512337. AB gratefully acknowledges financial support from PRF/ACS 270953 (37194-AC2) grant to H. D. Holland, Harvard University. Constructive reviews by M. Schidlowski, R. A. Fuck, A. C. Pedrosa-Soares, and G. Dix are acknowledged with thanks.

References

Akhmedov, A. M., 1990, Epochs of evaporization in the Paleoproterozoic of the Baltic Shield: Doklady Akademii Nauk, v. 312(3), p. 698–702.

Alkmim, F. F., and Marshak, S., 1998, Transamazonian Orogeny in the Southern São Francisco Craton Region, Minas Gerais, Brazil: evidence for Paleoproterozoic collision and collapse in the Quadrilátero Ferrífero: Precambrian Research, v. 90, p. 29–58.

Altermann, W., and Hälbich, I. W., 1991, Structural history of the southwestern corner of the Kaapvaal Craton and the adjacent Namaqua realm: new observations and a reappraisal: Precambrian Research, v. 52, p. 133–166.

Amelin, Y. V., Heaman, L .M., and Semenov, V. S., 1995, U-Pb geochronology of layered intrusions in the eastern Baltic Shield: implications for the timing and duration of Paleoproterozoic continental rifting: Precambrian Research, v. 75, p. 31–46.

Aspler, L. B., and Chiarenzelli, J. R., 1998, Two Neoarchean supercontinents? Evidence from the Paleoproterozoic: Sedimentary Geology, v. 120, p. 75–104.

Aspler, L. B., Cousens, B. L., and Chiarenzelli, J. R., 2002, Griffin gabbro sills (2.11 Ga), Hurwitz Basin, Nunavut, Canada: long-distance lateral transport of magmas in western Churchill Province crust: Precambrian Research, v. 117, p. 269–294.

Babinski, M., Chemale, F., Jr., and Van Schmus, W. R., 1995, The Pb/Pb age of the Minas Supergroup carbonate rocks, Quadrilátero Ferrífero, Brazil: Precambrian Research, v. 72, p. 235–245.

Banner, J. L., and Hanson, G. N., 1990, Calculation of simultaneous isotopic and trace element variations during water-rock interaction with applications to carbonate diagenesis: Geochimica et Cosmochimica Acta, v. 54, p. 3123–3137.

Barley, M. E., Pickard, A. L., and Sylvester, P. J., 1997, Emplacement of a large igneous province as a possible cause of banded iron formation 2.45 billion years ago: Nature, v. 385, p. 55–58.

Bartley, J. K., Semikhatov, M. A., Kaufman, A. J., Knoll, A. H., Pope, M. C., and Jacobsen, S. B., 2001, Global events across the Mesoproterozoic-Neoproterozoic boundary: C and Sr isotopic evidence from Siberia: Precambrian Research, v. 111, p. 165–202.

Baumgartner, L. P., and Valley, J. W., 2001, Stable Isotope Transport and Contact Metamorphic Fluid Flow, *in* Valley, J. W., and Cole, D. R., editors, Stable Isotope Geochemistry: Mineralogical Society of America and Geochemical Society Reviews in Mineralogy and Geochemistry, v. 43, p. 415–467.

Bekker, A., and Eriksson, K. A., 2003, Paleoproterozoic drowned carbonate platform on the southeastern margin of the Wyoming Craton: a record of the Kenorland breakup: Precambrian Research, v. 120, p. 327–364.

Bekker, A., and Karhu, J. A., 1996, Study of carbon isotope ratios of the early Proterozoic Snowy Pass Supergroup, WY and its application for correlation with the Chocolay Group, MI and the Huronian Supergroup, ON: Cable, Wisconsin, Institute on Lake Superior Geology, 42nd Annual Meeting, Proceedings, v. 42, part 1, p. 4–5.

——— 1997, Bimodality in carbon isotope values of dolomites of the Chocolay Group: possible implication for their age: Geological Society of America, Annual Meeting, Abstracts with Programs, v. 29, n. 4, p. 4.

Bekker, A., Karhu, J. A., and Eriksson, K. A., 1997, Paleoenvironmental changes at the end of the Paleoproterozoic carbon isotope excursion (~2.06 Ga): Geological Society of America, Annual Meeting, Abstracts with Programs, v. 29, n. 6, p. A– 467.

Bekker, A., Eriksson, K. A., Kaufman, A. J., Karhu, J. A., and Beukes, N. J., 1999, Paleoproterozoic record of biogeochemical events and ice ages: Geological Society of America, Annual Meeting, Abstracts with Programs, v. 31, n. 7, p. A– 487.

Bekker, A., Kaufman, A. J., Karhu, J. A., Beukes, N. J., Swart, Q. D., Coetzee, L. L., and Eriksson, K. A., 2001a, Chemostratigraphy of the Paleoproterozoic Duitschland Formation, South Africa: Implications for coupled climate change and carbon cycling: American Journal of Science, v. 301, p. 261–285.

Bekker, A., Master, S., Karhu, J. A., and Verhagen, B.T., 2001b, Chemostratigraphy of the Paleoproterozoic Magondi Supergroup, Zimbabwe: Houston, Lunar and Planetary Institute, 11th Annual V. M. Goldschmidt Conference, Abstract 3772, Lunar Planetary Institute Contribution 1088, (CD-ROM).

Bekker, A., Krapež, B., and Karhu, J. A., 2002, Preliminary chemostratigraphic data on carbonates from the Paleoproterozoic Turee Creek Supersequence and Wooly Dolomite of Western Australia: 16th International Sedimentologic Congress Abstract Volume, p. 26–27.

Bekker, A., Karhu, J. A., Eriksson, K. A., and Kaufman, A. J., 2003, Chemostratigraphy of Paleoproterozoic carbonate successions of the Wyoming Craton: tectonic forcing of biogeochemical change?: Precambrian Research, v. 120, p. 279–325.

Bertrand, J. M., and Jardim de Sá, E. F., 1990, Where are the Eburnian-Transamazonian collisional belts?: Canadian Journal of Earth Sciences, v. 27, p. 1382–1393.

Bidigare, R. R., Hanson, K. L., Buesseler, K. O., Wakeham, S. G., Freeman, K. H., Pancost, R. D., Millero, F. J., Steinberg, P., Popp, B. N., Latasa, M., Landry, M. R., and Laws, E. A., 1999, Iron-stimulated changes in ^{13}C fractionation and export by equatorial Pacific phytoplankton: Toward a paleogrowth rate proxy: Paleoceanography, v. 14, p. 589–595.

Botz, R., Stoffers, P., Faber, E., and Tietze, K., 1988, Isotope geochemistry of carbonate sediments from Lake Kivu (East-Central Africa): Chemical Geology, v. 69, p. 299–308.

Bowring, S. A., and Grotzinger, J. P., 1992, Implications of new chronostratigraphy for tectonic evolution of Wopmay Orogen, Northwest Canadian Shield: American Journal of Science, v. 292, p. 1–20.

Brasier, M. D., and Lindsay, J. F., 1998, A billion years of environmental stability and the emergence of eukaryotes: New data from Northern Australia: Geology, v. 26, p. 555–558.

Broecker, W. S., 1970, A boundary condition on the evolution of atmospheric oxygen: Journal of Geophysical Research, v. 75, p. 3553–3557.

Buick, I. S., Uken, R., Gibson, R. L., and Wallmach, T., 1998, High-$\delta^{13}C$ Paleoproterozoic carbonates from the Transvaal Supergroup, South Africa: Geology, v. 26, p. 875–878.

Burdett, J. W., Grotzinger, J. P., and Arthur, M. A., 1990, Did major changes in the stable-isotope composition of Proterozoic seawater occur?: Geology, v. 18, p. 227–230.

Carson, C. J., Ague, J. J., and Coath, C. D., 2002, U-Pb geochronology from Tonagh Island, East Antarctica: implications for the timing of ultra-high temperature metamorphism of the Napier Complex: Precambrian Research, v. 116, p. 237–263.

Chandler, F. W., 1988, Diagenesis of sabkha-related, sulphate nodules in the Early Proterozoic Gordon Lake Formation, Ontario, Canada: Carbonates and evaporites, v. 3, n. 1, p. 75–94.

Chemale, F., Jr., Rosière, C. A., and Endo, I., 1994, The tectonic evolution of the Quadrilátero Ferrífero, Minais Gerais, Brazil: Precambrian Research, v. 65, p. 25–54.

Claypool, G. E., and Kaplan, I. R., 1974, The origin and distribution of methane in marine sediments, *in* Kaplan, I. R., editor, Natural gases in Marine Sediments: New York, Plenum, p. 99–139.

Coetzee, L. L., ms, 2001, Genetic stratigraphy of the Paleoproterozoic Pretoria Group in the Western Transvaal: M.S. thesis, Rand Afrikaans University, Johannesburg, 212 p.

Daly, S. J., and Fanning, C. M., 1993, Archaean, *in* Drexel, J. F., Preiss, W. V., and Parker, A. J., editors, The geology of South Australia: Geological Survey of South Australia Bulletin, v. 54, n. 1, The Precambrian, p. 33–49.

Dardenne, M. A., and Campos Neto, M. C., 1975, Estromatólitos colunares na Série Minas (MG): Revista Brasileira de Geociências, v. 5, n. 2, p. 99–105.
Derry, L. A., Kaufman, A. J., and Jacobsen, S. B., 1992, Sedimentary cycling and environmental change in the late Proterozoic: evidence from stable and radiogenic isotopes: Geochimica et Cosmochimica Acta, v. 56, p. 1317–1329.
Dickens, G. R., Castillo, M. M., and Walker, J. C. G., 1997, A blast of gas in the latest Paleocene: simulating first-order effects of massive dissociation of oceanic methane hydrate: Geology, v. 25, p. 259–262.
Dix, G. R., Thomson, M. L., Longstaffe, F. J., and McNutt, R. H., 1995, Systematic decrease of high $\delta^{13}C$ values with burial in late Archaean (2.8 Ga) diagenetic dolomite: evidence for methanogenesis from the Crixás Greenstone Belt, Brazil: Precambrian Research, v. 70, p. 253–268.
Dorr, J. V. N.d., 1969, Physiographic, stratigraphic and structural development of the Quadrilátero Ferrífero, Minais Gerais, Brazil: United States Geological Survey Professional Paper 641-A, 110 p.
El Tabakh, M., Grey, K., Pirajno, F., and Schreiber, B. C., 1999, Pseudomorphs after evaporitic minerals interbedded with 2.2 Ga stromatolites of the Yerriba basin, Western Australia: Origin and significance: Geology, v. 27, p. 871–874.
Endo, I., Hartmann, L. A., Suita, M. T. F., Santos, J. O. S., Frantz, J. C., McNaughton, N. J., Barley, M. E., and Carneiro, M. A., 2002, Zircon SHRIMP isotopic evidence for Neoarchaean age of the Minas Supergroup, Quadrilátero Ferrífero, Minas Gerais: Congresso Brasileiro de Geologia, Sociedade Brasileira de Geologia, João Pessoa, Anais, p. 518.
Faure, G., and Powell, J. L., 1972, Strontium isotope geology: Berlin-Heidelberg, Springer-Verlag, 171 p.
Fortes, P. T. F. O., and Jost, H., 1996, Metallogeny of Mina III, Mina Nova and Mina Inglesa gold deposits, Crixás Greenstone Belt, Central Brazil: Symposium: Archaean Terranes of the South American Platform, Sociedade Brasileira de Geologia, Brasília, Brazil, p. 18–19.
Fortes, P. T. F. O., Pimental, M. M., Santos, R. V., and Junges, S. L., 2003, Sm-Nd studies at Mina III gold deposit, Crixás Greenstone Belt, Central Brazil: Implications for the depositional age of the upper metasedimentary rocks and associated Au mineralization: Journal of South American Earth Sciences, v. 16, n. 6, p. 471–480.
Fralick, P., Davis, D. W., and Kissin, S. A., 2002, The age of the Gunflint Formation, Ontario, Canada: single zircon U-Pb age determinations from reworked volcanic ash: Canadian Journal of Earth Sciences, v. 39, p. 1085–1091.
Friedman, I., and Murata, K. J., 1979, Origin of dolomite in Miocene Monterey Shale and related formations in the Temblor Range, California: Geochimica et Cosmochimica Acta, v. 43, p. 1357–1365.
Friedman, I., and O'Neil, J. R., 1977, Compilation of stable isotope fractionation factors of geochemical interest, *in* Fleischer, M., editor, Data of Geochemistry 6th edition: United States Geological Survey Professional Paper 440-KK.
Gair, J. E., 1962, Geology and ore deposits of the Nova Lima and Rio Aima Quadrangles Minas Gerais, Brazil: United States Geological Survey Professional Paper 341-A, 67 p.
Garcia, A. J. V., Fonseca, M. A., Bernardi, A. V., and Januzzi, A., 1988, Contribuição ao reconhecimento dos paleoambientes deposicionais do grupo Piracicaba na região de Dom Bosco - SW de Ouro Preto, Quadrilátero Ferrífero-MG: Acta Geologica Leopoldensia, v. 11, n. 27, p. 83–108.
Genest, S., 1985, Aphebian evaporites and related red beds in Peribonca Formation (Otish Group, Central Quebec): evidence for coastal sabkha and subaqueous environments: Geological Association of Canada / Mineralogical Association of Canada abstracts, v. 10, p. A21.
Gorokhov, I. M., Kuznetsov, A. B., Melezhik, V. A., Konstantinova, G. V., and Melnikov, N. N., 1998, Sr Isotopic Composition in the Upper Jatulian (Early Proterozoic) Dolomites of the Tulomozero Formation, Southeastern Karelia: Doklady Akademii Nauk, v. 360, p. 533–536.
Gregg, J. M., and Sibley, D. F., 1984, Epigenetic dolomitization and the origin of xenotopic dolomite texture: Journal of Sedimentary Petrology, v. 54, p. 908–931.
Hannah, J. L., Stein, H. J., Bekker, A., Markey, R. J., and Holland, H. D., 2003, Chondritic Initial $^{187}Os/^{188}Os$ in Paleoproterozoic shale (seawater) and the onset of oxidative weathering: Geochimica et Cosmochimica Acta, v. 67, A-34.
Hayes, J. M., 1994, Global methanotrophy at the Archean-Proterozoic transition, *in* Bengston, S., editor, Early Life on Earth: New York, Columbia University Press, p. 220–236.
Hayes, J. M., Kaplan, I. R., and Wedeking, K. W., 1983, Precambrian organic geochemistry, preservation of the record, *in* Schopf, J. W., editor, The Earth's earliest biosphere: its origin and evolution: Princeton, Princeton University Press, p. 93–134.
Hayes, J. M., Strauss, H., and Kaufman, A. J., 1999, The abundance of ^{13}C in marine organic matter and isotopic fractionation in the global biogeochemical cycle of carbon during the past 800 Ma: Chemical Geology, v. 161, p. 103–125.
Heaman, L. M., 1997, Global mafic volcanism at 2.45 Ga: Remnants of an ancient large igneous province?: Geology, v. 25, p. 299–302.
Hemzacek, J. M., Perry, E. C., Larue, D. K., and Feng, J., 1982, Sulfur isotope composition of sulfate in chert horizons of the Proterozoic (Precambrian X) Kona Dolomite, Marquette Region, Michigan: Geological Society of America Abstracts with Programs, v. 14, n. 7, p. 512.
Hennessy, J., and Knauth, L. P., 1985, Isotopic variations in dolomite concretions from the Monterey Formation, California: Journal of Sedimentary Petrology, v. 55, p. 120–130.
Herz, N., 1962, Chemical composition of Precambrian pelitic rocks, Quadrilátero Ferrífero, Minas Gerais, Brazil: United States Geological Survey Professional Paper 450-C, p. C75–C78.
——— 1978, Metamorphic rocks of the Quadrilátero Ferrífero, Minas Gerais, Brazil: United States Geological Survey Professional Paper 641-C, 81 p.

Herz, N., and Dutra, C. V., 1964, Geochemistry of some kyanites from Brazil: The American Mineralogist, v. 49, p. 1290–1305.
Hoffman, P. F., 1991, Did the breakup of Laurentia turn Gondwanaland inside-out?: Science, v. 252, p. 1409–1412.
Hoffman, P. F., and Schrag, D. P., 2000, Snowball Earth: Scientific American, v. 282, p. 68–75.
——— 2002, The Snowball Earth hypothesis: testing the limits of global change: Terra Nova, v. 14, p. 129–155.
Hoffman, P. F., Kaufman, A. J., Halverson, G. P., and Schrag, D. P., 1998, A Neoproterozoic Snowball: Earth: Science, v. 281, p. 1342–1346.
Irwin, H., Curtis, C., and Coleman, M., 1977, Isotopic evidence for source of diagenetic carbonates formed during burial of organic-rich sediments: Nature, v. 269, p. 209–213.
Jahren, A. H., Arens, N. C., Sarmiento, G., Guerrero, J., and Amundson, R., 2001, Terrestrial record of methane hydrate dissociation in the Early Cretaceous: Geology, v. 29, p. 159–162.
Johnson, R. F., 1962, Geology and ore deposits of the Cachoeira do Campo Dom Bosco, and Ouro Branco Quadrangles, Minas Gerais, Brazil: United States Geological Survey Professional Paper 341-B, p. B1–B-39.
Kah, L. C., Sherman, A. G., Narbonne, G. M., Knoll, A. H., and Kaufman, A. J., 1999, $\delta^{13}C$ stratigraphy of the Proterozoic Bylot Supergroup, Baffin Island, Canada: implications for regional lithostratigraphic correlations: Canadian Journal of Earth Sciences, v. 36, p. 313–332.
Kamber, B. S., and Webb, G. E., 2001, The geochemistry of late Archaean microbial carbonate; Implications for ocean chemistry and continental erosion history: Geochimica et Cosmochimica Acta, v. 65, p. 2509–2525.
Karhu, J. A., 1993, Paleoproterozoic evolution of the carbon isotope ratios of sedimentary carbonates in the Fennoscandian Shield: Geological Survey of Finland Bulletin 371, 87 p.
Karhu, J. A., and Holland, H. D., 1996, Carbon isotopes and the rise of atmospheric oxygen: Geology, v. 24, p. 867–870.
Karhu, J. A., and Melezhik, V. A., 1992, Carbon isotope systematics of early Proterozoic sedimentary carbonates in the Kola Peninsula, Russia: correlations with Jatulian formations in Karelia, *in* Balagansky, V. V., and Mitrofanov, F. P., editors, Correlation of Precambrian formations of the Kola-Karelia Region and Finland: Apatity, Kola Scientific Centre of the Russian Academy of Sciences, p. 48–53.
Kasting, J. F., 1998, Methane in the early atmosphere of the Earth: Mineralogical Magazine, v. 62A, p. 751–752.
Kaufman, A. J., 1997, An ice age in the tropics: Nature, v. 386, p. 227–228.
Kaufman, A. J., and Knoll, A. H., 1995, Neoproterozoic variations in the C-isotopic composition of seawater: stratigraphic and biogeochemical implications: Precambrian Research, v. 73, p. 27–49.
Kaufman, A. J., Hayes, J. M., Knoll, A. H., and Germs, G. J. B., 1991, Isotope compositions of carbonates and organic carbon from upper Proterozoic successions in Namibia: Stratigraphic variation and the effects of diagenesis and metamorphism: Precambrian Research, v. 49, p. 301–327.
Kaufman, A. J., Knoll, A. H., and Narbonne, G. M., 1997, Isotopes, ice ages, and terminal Proterozoic Earth history: National Academy of Science Proceedings, 94, p. 6600–6605.
Kohonen, J., 1995, From continental rifting to collisional crustal shortening – Paleoproterozoic Kaleva metasediments of the Höytiäinen area in North Karelia, Finland: Geological Survey of Finland Bulletin 380, 79 p.
Krapež, B., 1996, Sequence-stratigraphic concepts applied to the identification of basin-filling rhythms in Precambrian successions: Australian Journal of Earth Sciences, v. 43, p. 355–380.
Kump, L. R., Kasting, J. F., and Barley, M. E., 2000, The rise of atmospheric oxygen and the "upside down" Archean mantle: Geochemistry, Geophysics, Geosystems, v. 2, Paper no. 2000GC000114.
Kuznetsov, A. B., Melezhik, V. A., Gorokhov, I. M., Mel'nikov, N. N., and Fallick, A. E., 2003, Sr Isotope Composition in Paleoproterozoic Carbonates Extremely Enriched in ^{13}C: Kaniapiskau Supergroup, the Labrador Trough of the Canadian Shield: Stratigraphy and Geological Correlation, v. 11(3), p. 209–219.
Lindsay, J. F., and Brasier, M. D., 2002, Did global tectonics drive early biosphere evolution? Carbon isotope record from 2.6 to 1.9 Ga carbonates of western Australian basins: Precambrian Research, v. 114, p. 1–34.
Logan, B. W., Rezak, R., and Ginsburg, R. N., 1964, Classification and environmental significance of algal stromatolites: Journal of Geology, v. 72, p. 68–83.
Machado, N., and Carneiro, M. A., 1992, U-Pb evidence of late Archean tectono-thermal activity in the southern São Francisco shield, Brazil: Canadian Journal of Earth Sciences, v. 29, p. 2341–2346.
Machado, N., Noce, C. M., Ladeira, E. A., and Belo de Oliveira, O., 1992, U-Pb geochronology of Archean magmatism and Proterozoic metamorphism in the Quadrilátero Ferrífero, southern São Francisco craton, Brazil: Geological Society of America Bulletin, v. 104, p. 1221–1227.
Machado, N., Schrank, A., Noce, C. M., and Gauthier, G., 1996, Ages of detrital zircon from Archean-Paleoproterozoic sequences: implications for greenstone belt setting and evolution of a Transamazonian foreland basin in Quadrilátero Ferrífero, southeast Brazil: Earth and Planetary Science Letters, v. 141, p. 259–276.
Marshak, S., and Alkmim, F. F., 1989, Proterozoic contraction/extension tectonics of the southern São Francisco region, Minas Gerais, Brazil: Tectonics, v. 8, p. 555–571.
Marshak, S., Alkmim, F. F., and Jordt-Evangelista, H., 1992, Proterozoic crustal extension and the generation of dome-and-keel structures in an Archaean granite-greenstone terrane: Nature, v. 357, p. 491–493.
Martin, D. M., Clendenin, C. W., Krapež, B., and McNaughton, N. J., 1998, Tectonic and geochronological constraints on late Archaean and Palaeoproterozoic stratigraphic correlation within and between the Kaapvaal and Pilbara Cratons: Journal of the Geological Society London, v. 155, p. 311–322.

Master, S., 1990, Oldest evaporites in Africa: 2.06 Ga continental playa deposits of the Deweras Group, Zimbabwe: Université Nancy I, 15th Colloquim of African Geology, p. 103.
Master, S., Verhagen, B. T., and Duane, M. J., 1990, Isotopic signatures of continental and marine carbonates from the Magondi Belt, Zimbabwe: Implications for the global carbon cycle at 2.0 Ga: 23rd Earth Science Congress, Geological Society of South Africa Abstracts, p. 346–348.
Maxwell, C. H., 1972, Geology and ore deposits of the Alegria District, Minas Gerais, Brazil: United States Geological Survey Professional Paper 341-J, 72 p.
McCrea, J. M., 1950, On the isotope chemistry of carbonates and a paleotemperature scale: Journal of Chemical Physics, v. 18, p. 849–857.
Melezhik, V. A., and Fallick, A. E., 1996, A widespread positive $\delta^{13}C_{carb}$ anomaly at around 2.33-2.06 Ga on the Fennoscandian Shield: a paradox?: Terra Nova, v. 8, p. 141–157.
Melezhik, V. A., and Fetisova, O. A., 1989, First discovery of syngenetic barites in the Precambrian of the Baltic Shield: Doklady Akademii Nauk, v. 307, p. 422–425.
Melezhik, V. A., and Sturt, B. A., 1994, General geology and evolutionary history of the early Proterozoic Polmak-Pasvik-Pechenga-Imandra/Varzuga-Ust' Ponoy Greenstone Belt in the northeastern Baltic Shield: Earth Science Reviews, v. 36, p. 205–241.
Melezhik, V. A., Fallick, A. E., Makarikhin, V.V., and Lyubtsov, V. V., 1997a, Links between Paleoproterozoic palaeogeography and rise and decline of stromatolites: Fennoscandian Shield: Precambrian Research, v. 82, p. 311–348.
Melezhik, V. A., Fallick, A. E., and Clark, T., 1997b, Two billion year old isotopically heavy carbon: evidence from the Labrador Trough, Canada: Canadian Journal of Earth Sciences, v. 34, p. 271–285.
Melezhik, V. A., Fallick, A. E., Medvedev, P. V., and Makarikhin, V. V., 1999, Extreme $\delta^{13}C_{carb}$ enrichment in ca. 2.0 Ga magnesite-stromatolite-dolomite-'red beds' association in a global context: a case for the worldwide signal enhanced by a local environment: Earth Science Reviews, v. 48, p. 71–120.
Minter, W. E. L., Renger, F. E., and Siegers, A., 1990, Early Proterozoic gold placers of the Moeda Formation within the Gandarela syncline, Minas Gerais, Brazil: Economic Geology, v. 85, p. 943–951.
Mirota, M. D., and Veizer, J., 1994, Geochemistry of Precambrian Carbonates: IV. Aphebian Albanel Formations, Quebec, Canada: Geochimica et Cosmochimica Acta, v. 58, p. 1735–1745.
Moore, S. L., 1969, Geology and ore deposits of the Antônio dos Santos, Gongo Sôco and Conceição do Rio Acima Quadrangles, Minas Gerais, Brazil: United States Geological Survey Professional Paper 341-I, 50 p.
Nelson, D. R., Trendall, A. F., and Altermann, W., 1999, Chronological correlations between the Pilbara and Kaapvaal cratons: Precambrian Research, v. 97, p. 165–189.
Noce, C. M., Machado, N., and Teixeira, W., 1998, U-Pb geochronology of gneisses and granitoids in the Quadrilátero Ferrífero (southern São Francisco Craton): age constraints from Archean and Paleoproterozoic magmatism and metamorphism: Revista Brasileira de Geociências, v. 28, p. 95–102.
Ojakangas, R. W., 1988, Glaciation: an uncommon "mega-event" as a key to intracontinental and intercontinental correlation of Paleoproterozoic basin fills, North American and Baltic cratons, *in* Kleinspehn, K. L., and Paola, C., editors, New perspectives in basin analysis: New York, Springer-Verlag, p. 431–444.
Page, R. W., and Sweet, I. P., 1998, Geochronology of basin phases in the western Mt Isa Inlier, and correlation with the McArthur Basin: Australian Journal of Earth Sciences, v. 45, p. 219–232.
Pavlov, A. A., Kasting, J. F., and Brown, L. L., 2000, Greenhouse warming by CH_4 in the atmosphere of early Earth: Journal of Geophysical Research, v. 105, p. 11981–11990.
Pickard, A. L., 2002, SHRIMP U-Pb zircon ages of tuffaceous mudrocks in the Brockman Iron Formation of the Hamersley Range, Western Australia: Australian Journal of Earth Sciences, v. 49, p. 491–507.
Pickard, A. L., 2003, SHRIMP U Pb zircon cages for the Paleoproterzoic Kuruman Iron Formation, Northern Cape Province, South Africa: evidence for simultaneous BIF deposition on Kaapvaal and Pilbara Cratons: Precambrian Research, v. 125, p. 275–315.
Pidgeon, R. T., and Horwitz, R. C., 1991, The origin of olistoliths in Proterozoic rocks of the Ashburton Trough, Western Australia, using zircon U-Pb isotopic characteristics: Australian Journal of Earth Sciences, v. 38, p. 55–63.
Pokrovsky, B. G., and Melezhik, V. A., 1995, Variations of oxygen and carbon isotopes in Paleoproterozoic carbonate rocks of the Kola Peninsula: Stratigraphy and Geological Correlation, v. 3, n. 5, p. 42–53.
Popp, B. N., Laws, E. A., Bidigare, R. R., Dore, J. E., Hanson, K. L., and Wakeham, S. G., 1998, Effect of phytoplankton cell geometry on carbon isotopic fractionation: Geochimica et Cosmochimica Acta, v. 62, p. 69–77.
Renger, F. E., Noce, C. M., Romano, A. W., and Machado, N., 1994, Evolução sedimentar do Supergrupo Minas: 500Ma de registro geológico no Quadrilátero Ferrífero, Minas Gerais, Brasil: Geonomos, v. 2, n. 1, p. 1–11.
Roberts, H., Dahl, P. S., Kelley, S., and Frei, R., 2002, New ^{207}Pb-^{206}Pb and ^{40}Ar-^{39}Ar ages from SW Montana, USA: constraints on the Proterozoic and Archaean tectonic and depositional history of the Wyoming Province: Precambrian Research, v. 117, p. 119–143.
Rohon, M. L., Vialette, Y., Clark, T., Roger, G., Ohnenstetter, D., and Vidal, P., 1993, Aphebian mafic-ultramafic magmatism in the Labrador Trough (New Quebec): its age and the nature of its mafic source: Canadian Journal of Earth Sciences, v. 30, p. 1582–1593.
Romano, A. W., ms, 1989, Evolution tectonique de la region Nord-Ouest du Quadrilatere Ferrifere – Minas Gerais – Bresil (Geochronologie du socle – aspects geochimiques et petrographiques des supergroupes Rio Das Velhas et Minas): Ph.D. thesis, Université de Nancy I, Nancy, France, 259 p.
Rosenbaum, J., and Sheppard, S. M. F., 1986, An isotopic study of siderites, dolomites and ankerites at high temperatures: Geochimica et Cosmochimica Acta, v. 50, p. 1147–1150.
Rye, R., and Holland, H. D., 2000, Life associated with a 2.76 Ga ephemeral pond?: evidence from Mount Roe #2 paleosol: Geology, v. 28, p. 483–486.

Sansone, F. J., Tribble, G. W., Andrews, C. C., and Chanton, J. P., 1990, Anaerobic diagenesis within Recent, Pleistocene, and Eocene marine carbonate frameworks: Sedimentology, v. 37, p. 997–1009.
Schidlowski, M., and Todt, W., 1998, The Proterozoic Lomagundi carbonate province as paragon of a ^{13}C-enriched carbonate facies: geology, radiometric age and geochemical significance: Chinese Science Bulletin, v. 43, p. 114.
Schidlowski, M., Eichmann, R., and Junge, C. E., 1975, Precambrian Sedimentary Carbonates: Carbon and oxygen isotope geochemistry and implications for the terrestrial oxygen budget: Precambrian Research, v. 2, p. 1–69.
Schidlowski, M., Eichmann, R., and Fiebiger, W., 1976a, Isotopic fractionation between organic carbon and carbonate carbon in Precambrian banded ironstone series from Brazil: Neues Jahrbuch fur Mineralogie, Monatshefte, v. 8, p. 344–353.
Schidlowski, M., Eichmann, R., and Junge, C. E., 1976b, Carbon isotope geochemistry of the Precambrian Lomagundi carbonate province, Rhodesia: Geochimica et Cosmochimica Acta, v. 40, p. 449–455.
Sial, A. N., Ferreira, V. P., Romano, A. W., de Almeida, A. R., and Parente, C. V., 1999, Carbon and oxygen isotope variations in some Paleo- to Neoproterozoic carbonate sequences from Brazil: Cordoba, Argentina, Actas II South American Symposium on Isotope Geology, p. 449–452.
Sial, A. N., Ferreira, V. P., de Almeida, A. R., Romano, A. W., Parente, C. V., Da Costa, M. L., and Santos, V. H., 2000, Carbon isotope fluctuations in Precambrian carbonate sequences of several localities in Brazil: Anais da Academia Brasileira de Ciencias, v. 72, n. 4, p. 539–558.
Simmons, G. C., 1968, Geology and iron deposits of the Western Serra do Curral, Minas Gerais, Brazil: United States Geological Survey Professional Paper 341-G, 57 p.
Souza, P. C., and Müller, G., 1984, Primeiras Estruturas Algais Comprovadas na Formação Gandarela, Quadrilátero Ferrífero: Revista Escola de Minas Ouro Preto, v. 2, p. 13–21.
Stiller, M., Rounick, J. S., and Shasha, S., 1985, Extreme carbon-isotope enrichments in evaporating brines: Nature, v. 316, p. 434–435.
Sturt, B. A., Melezhik, V. A., and Ramsay, D. M., 1994, Early Proterozoic regolith at Pasvik, NE Norway: palaeoenvironmental applications for the Baltic Shield: Terra Nova, v. 6, p. 618–633.
Sumner, D. Y., and Bowring, S. A., 1996, U-Pb geochronologic constraints on deposition of the Campbellrand Subgroup, Transvaal Supergroup, South Africa: Precambrian Research, v. 79, p. 25–35.
Swart, Q. D., ms, 1999, Carbonate rocks of the Paleoproterozoic Pretoria and Postmasburg Groups, Transvaal Supergroup: M.S. thesis, Rand Africaans University, Johannesburg, South Africa, 126 p.
Talbot, M. R., and Kelts, K., 1986, Primary and diagenetic carbonates in the anoxic sediments of Lake Bosumtwi, Ghana: Geology, v. 14, p. 912–916.
Taylor, A. E., and Lasaga, A. C., 1999, The role of basalt weathering in the Sr isotope budget of the oceans: Chemical Geology, v. 161, p. 199–214.
Thorpe, R. I., Cumming, G. L., and Krstic, D., 1984, Lead isotope evidence regarding age of gold deposits in the Nova Lima District, Minas Gerais, Brazil: Revista Brasileira de Geociências, v. 14, p. 147–152.
Tikhomirova, M., and Makarikhin, V. V., 1993, Possible reasons for the $\delta^{13}C$ anomaly of lower Proterozoic sedimentary carbonates: Terra Nova, v. 5, p. 244–248.
Trendall, A. F., Nelson, D. R., de Laeter, J. R., and Hassler, S. W., 1998, Precise zircon U-Pb ages from the Marra Mamba Iron Formation and Wittenoom Formation, Hamersley Group, Western Australia: Australian Journal of Earth Sciences, v. 45, p. 137–142.
Valley, J. W., 1986, Stable isotope geochemistry of metamorphic rocks, *in* Valley, J. W., Taylor, H. P., and O'Neil, J. R., editors, Stable isotopes in high temperature geological processes: Mineralogical Society of America Reviews in Mineralogy, v. 16, p. 445–489.
Vasil'eva, I. M., Ovchinnikova, G. V., Melezhik, V. A., Gorokhov, I. M., Kuznetsov, A. B., and Gorokhovskii, B. M., 2000, Pb-Pb age of carbonate rocks of the Tulomozerskaya Formation, Northern Onega Lake Region, *in* Negrutza, T. F., and Negrutza, V. Z., editors, Proceedings III All-Russia Conference "General Issues of Precambrian subdivision": Apatity, p. 53–54.
Veizer, J., 1983, Chemical diagenesis of carbonates: Theory and application of trace element technique, *in* Arthur, M. A., Anderson, T. F., Kaplan, I. R., Veizer, J., and Land, L. S., editors, Stable isotopes in Sedimentary Geology: Society of Economic Paleontologists and Mineralogists, Short Course 10, p. 3-1–3-100.
——— 1994, The Archean-Proterozoic transition and its environmental implications, *in* Bengston, S., editor, Early Life on Earth. Nobel Symposium No. 84: New York, Columbia University Press, p. 208–219.
Veizer, J., Hoefs, J., Lowe, D. R., and Thurston, P. C., 1989a, Geochemistry of Precambrian carbonates: II. Archean greenstone belts and Archean sea water: Geochimica et Cosmochimica Acta, v. 53, p. 859–871.
Veizer, J., Hoefs, J., Ridler, R. H., Jensen, L. S., and Lowe, D. R., 1989b, Geochemistry of Precambrian carbonates: I. Archean hydrothermal systems: Geochimica et Cosmochimica Acta, v. 53, p. 845–857.
Veizer, J., Clayton, R. N., Hinton, R. W., Von Burn, V., Mason, T. R., Buck, S. G., and Hoefs, J., 1990, Geochemistry of Precambrian carbonates: 3-shelf seas and non-marine environments of the Archean: Geochimica et Cosmochimica Acta, v. 54, p. 2717–2729.
Veizer, J., Clayton, R. N., and Hinton, R. W., 1992a, Geochemistry of Precambrian Carbonates: IV. Early Paleoproterozoic (2.25 ± 0.25 Ga) seawater: Geochimica et Cosmochimica Acta, v. 56, p. 875–885.
Veizer, J., Plumb, K. A., Clayton, R. N., Hinton, R. W., and Grotzinger, J. P., 1992b, Geochemistry of Precambrian Carbonates: V. Late Paleoproterozoic Seawater: Geochimica et Cosmochimica Acta, v. 56, p. 2487–2501.
Villaça, J. N., and Moura, L. A. M., 1981, Uranium in the Precambrian Moeda Formation, Minas Gerais, Brazil: United States Geological Survey Professional Paper 1161-T, p. T1–T14.
Whittaker, S. G., Sami, T. T., Kyser, T. K., and James, N. P., 1998, Petrogenesis of 1.9 Ga limestones and dolostones and their record of Paleoproterozoic environments: Precambrian Research, v. 90, p. 187–202.
Williams, H., Hoffman, P. F., Lewry, J. F., Monger, J. W. H., and Rivers, T., 1991, Anatomy of North America: thematic geologic portrayals of the continent: Tectonophysics, v. 187, p. 117–134.

Winter, B. L., and Knauth, L. P., 1992a, Stable isotope geochemistry of carbonate fracture fills in the Monterey Formation, California: Journal of Sedimentary Petrology, v. 62, p. 208–219.

——— 1992b, Stable isotope geochemistry of early Proterozoic carbonate concretions in the Animikie Group of the Lake Superior region: evidence for anaerobic bacterial processes: Precambrian Research, v. 54, p. 131–151.

Young, G. M., 1973, Tillites and aluminous quartzites as possible time markers for middle Precambrian (Aphebian) rocks of North America, *in* Young, G. M., editor, Huronian Stratigraphy and Sedimentation: Geological Association of Canada Special Paper 12, p. 97–127.

Young, G. M., Long, D. G. F., Fedo, C. M., and Nesbitt, H. W., 2001, Paleoproterozoic Huronian basin: product of a Wilson cycle punctuated by glaciations and a meteorite impact: Sedimentary Geology, v. 141–142, p. 233–254.

Yudovich, Y. Y., Makarikhin, V. V., Medvedev, P. V., and Sukhanov, N. V., 1990, Carbon isotopic anomalies in carbonates of Karelian Series: Geochemistry, v. 7, p. 972–978.